Genome organization regulates nuclear pore complex formation and promotes differentiation during *Drosophila* oogenesis

Noor M. Kotb,[1,2,3] Gulay Ulukaya,[3,4] Ankita Chavan,[5] Son C. Nguyen,[6] Lydia Proskauer,[2,9] Eric F. Joyce,[6] Dan Hasson,[3,4,7,8] Madhav Jagannathan,[5] and Prashanth Rangan[3]

[1]Department of Biomedical Sciences/Wadsworth Center, University at Albany State University of New York (SUNY), Albany, New York 12202, USA; [2]Department of Biological Sciences/RNA Institute, University at Albany SUNY, Albany, New York 12202, USA; [3]Department of Cell, Developmental, and Regenerative Biology, Black Family Stem Cell Institute, Icahn School of Medicine at Mount Sinai, New York, NewYork 10029, USA; [4]Bioinformatics for Next-Generation Sequencing (BiNGS) Core, Tisch Cancer Institute, Icahn School of Medicine at Mount Sinai, New York, New York 10029, USA; [5]Institute of Biochemistry, Department of Biology, Eidgenössische Technische Hochschule (ETH) Zürich, 8092 Zürich, Switzerland; [6]Department of Genetics, University of Pennsylvania, Philadelphia, Pennsylvania 19104, USA; [7]Department of Oncological Sciences, Icahn School of Medicine at Mount Sinai, New York, New York 10029, USA; [8]Graduate School of Biomedical Sciences, Icahn School of Medicine at Mount Sinai, New York, New York 10029, USA

Genome organization can regulate gene expression and promote cell fate transitions. The differentiation of germline stem cells (GSCs) to oocytes in *Drosophila* involves changes in genome organization mediated by heterochromatin and the nuclear pore complex (NPC). Heterochromatin represses germ cell genes during differentiation, and NPCs anchor these silenced genes to the nuclear periphery, maintaining silencing to allow for oocyte development. Surprisingly, we found that genome organization also contributes to NPC formation, mediated by the transcription factor Stonewall (Stwl). As GSCs differentiate, Stwl accumulates at boundaries between silenced and active gene compartments. Stwl at these boundaries plays a pivotal role in transitioning germ cell genes into a silenced state and activating a group of oocyte genes and nucleoporins (Nups). The upregulation of these Nups during differentiation is crucial for NPC formation and further genome organization. Thus, cross-talk between genome architecture and NPCs is essential for successful cell fate transitions.

[*Keywords*: differentiation; genome organization; heterochromatin; nucleoporins; NPC; lamin; TAD; LAD]

Supplemental material is available for this article.

Received December 10, 2023; revised version accepted May 21, 2024.

During oogenesis, germline stem cells (GSCs) differentiate and undergo meiosis to generate oocytes (Seydoux and Braun 2006; Lehmann 2012; Lesch and Page 2012; Blatt et al. 2020). These oocytes accrue a maternally synthesized trust fund of RNAs, called maternal RNAs, required to launch the next generation (Spradling 1993; Navarro et al. 2004; Kugler and Lasko 2009; Blatt et al. 2020). *Drosophila* oogenesis has a well-characterized transition from GSC to oocyte (Fig. 1A,A1; McKearin and Spradling 1990; Chen and McKearin 2003a; Huynh and Johnston 2004; Spradling et al. 2011; Lehmann 2012). A programmatic transition, referred to as the germ cell-to-maternal transition (GMT), promotes the silencing of genes that are expressed during the early stages of oogenesis, including a cohort of differentiation-promoting genes (Fig. 1A1; DeLuca et al. 2020; Blatt et al. 2021; McCarthy et al. 2022; Sarkar et al. 2023). These "early oogenesis genes" include *ribosomal small subunit protein19b* (*rpS19b*) and *blanks* (Gerbasi et al. 2011; Blatt et al. 2021; McCarthy et al. 2022; Sarkar et al. 2023). The transcriptional silencing of these early oogenesis genes is mediated by SET domain bifurcated histone lysine methyltransferase 1 (SETDB1), which leads to methylation of H3K9 and thereby establishes heterochromatin (Rangan et al. 2011; Clough et al. 2014; Sarkar et al. 2023). Once

[9]Present address: Department of Biochemistry and Molecular Biology, University of Massachusetts Amherst, Amherst, MA 01003, USA.
Corresponding author: prashanth.rangan@mssm.edu
Article published online ahead of print. Article and publication date are online at http://www.genesdev.org/cgi/doi/10.1101/gad.351402.123. Freely available online through the *Genes & Development* Open Access option.

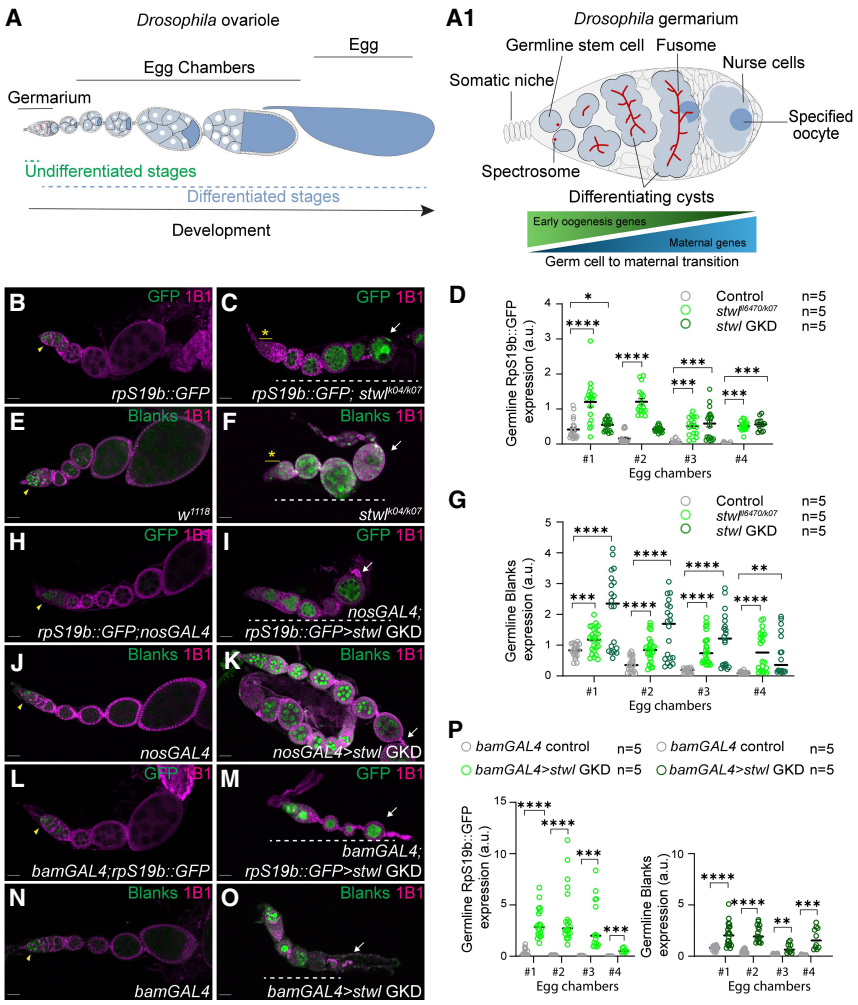

Figure 1. *stwl* is required for silencing RpS19b::GFP and Blanks during oogenesis. (*A*) A schematic of a *Drosophila* ovariole consisting of a germarium and egg chambers surrounded by somatic cells (white). Egg chambers grow and produce an egg (dark blue). (*A1*) A schematic of a *Drosophila* germarium. Germline stem cells (GSCs; blue) are proximal to the somatic niche (gray) and divide to give rise to daughter cells, called cystoblasts. Both GSCs and cystoblasts are marked by spectrosomes (red). Cystoblasts differentiate, giving rise to 2, 4, 8, and 16 cell cysts (blue), marked by fusomes (red). In the 16 cell cyst, one cell commits to meiosis and specifies an oocyte (dark blue), whereas the other 15 cells become nurse cells (light blue). Early oogenesis genes are expressed in the undifferentiated stages and are attenuated upon oocyte specification, while maternal genes increase and are enriched in the differentiated stages. This transition happens in a programmatic manner called the germ cell-to-maternal transition (GMT). Undifferentiated stages are spectrosome-containing germline stem cells and their daughter cystoblasts, while differentiated stages are cysts with specified oocytes. (*B*,*C*) Ovariole of control (*B*) and $stwl^{K04/K07}$ ovaries carrying *rpS19b::GFP* (*C*) stained for GFP (green) and 1B1 (magenta). In controls, GFP is expressed in the undifferentiated stages and early cysts and then silenced (yellow arrowheads). In *stwl* mutants, egg chambers ectopically expressed RpS19b::GFP (white dashed line), did not grow, and died during oogenesis. The yellow asterisk indicates loss of GSCs in $stwl^{K04/K07}$ ovaries. (*D*) Arbitrary unit (a.u.) quantification of RpS19b::GFP expression in egg chambers in $stwl^{k04/k07}$ ovaries and upon the germline knockdown (GKD) of *stwl* (green) compared with control ovaries (gray). Statistics were derived from two tailed *t*-tests. $n = 5$ ovarioles per genotype. (*) $P < 0.05$, (***) $P < 0.001$, (****) $P < 0.0001$. (*E*,*F*) Ovariole of control w^{1118} (*E*) and $Stwl^{K04/K07}$ (*F*) ovaries stained for Blanks (green) and 1B1 (magenta). Blanks is expressed in the undifferentiated cells (yellow arrowheads) and is attenuated in the egg chambers. *stwl* mutants resulted in egg chambers that ectopically expressed Blanks (white dashed line), did not grow, and died during oogenesis. The yellow asterisk indicates loss of GSCs in $stwl^{K04/K07}$ ovaries. (*G*) Arbitrary unit (a.u.) quantification of Blanks expression in egg chambers in $stwl^{k04/k07}$ ovaries and upon the GKD of *Stwl* (green) compared with control ovaries (gray). Statistics were derived from two tailed *t*-tests. $n = 5$ ovarioles per genotype. (**) $P < 0.01$, (***) $P < 0.001$, (****) $P < 0.0001$. (*H*,*I*) Ovariole of control *rpS19b::GFP;nosGAL4* (*H*) and GKD of *stwl* (*I*) stained for GFP (green) and 1B1 (magenta). In the controls, GFP is expressed in the undifferentiated cells (yellow arrowheads) and is attenuated in the egg chambers. *stwl* GKD resulted in egg chambers that ectopically expressed RpS19b::GFP (white dashed line), did not grow, and died during oogenesis. Quantitation of GFP levels in *stwl* GKD in *D*. (*J*,*K*) Ovariole of control (*J*) and GKD of *stwl* (*K*) ovaries stained for Blanks (green) and 1B1 (magenta). In the controls, Blanks is expressed in the undifferentiated cells (yellow arrowheads) and is attenuated in the egg chambers. *stwl* GKD resulted in egg chambers that ectopically expressed blanks (white dashed line), did not grow, and died during oogenesis. Quantitation of GFP levels in *stwl* GKD in *G*. (*L*,*M*) Ovariole of control *bamGAL4;rpS19b::GFP* (*L*) and *bamGAL4; rpS19b::GFP>stwl* GKD (*M*) ovaries stained for GFP (green) and 1B1 (magenta). In the controls, GFP is expressed in the undifferentiated cells (yellow arrowheads) and is attenuated in the egg chambers. *stwl* GKD in the cyst stages using *bamGAL4;rpS19b::GFP* resulted in egg chambers that ectopically expressed RpS19b::GFP (white dashed line), did not grow, and died during oogenesis. (*N*,*O*) Ovariole of control (*N*) and GKD of *stwl* in the cyst stages using *BamGAL4* (*O*) stained for Blanks (green) and 1B1 (magenta). In the controls, Blanks is expressed in the undifferentiated cells (yellow arrowheads) and is attenuated in the egg chambers. *stwl* GKD in the cyst stages resulted in egg chambers that ectopically expressed blanks (white dashed line), did not grow, and died during oogenesis. (*P*) Arbitrary unit (a.u.) quantification of early oogenesis proteins RpS19b::GFP and Blanks expression in egg chambers upon the GKD of *stwl* (green) compared with control ovaries (gray). Statistics were derived from two tailed *t*-tests. $n = 5$ ovarioles per genotype. (**) $P < 0.01$, (***) $P < 0.001$, (****) $P < 0.0001$. $n = 5$ ovarioles/germaria used for all quantifications in this study. Multiple cells from the ovarioles/germaria were used for the quantifications. Scale bars, 15 μm.

transcriptionally silenced, these heterochromatic regions containing early oogenesis genes are anchored to the nuclear periphery mediated by the nuclear pore complex (NPC) (Sarkar et al. 2023). Loss of SETDB1 or specific nucleoporins (Nups) that comprise the NPCs leads to the upregulation of early oogenesis genes in the egg chambers that fail to grow and result in sterility (Colozza et al. 2011; Clough et al. 2014; Sarkar et al. 2023). Silencing of these early oogenesis genes is concomitant with increased expression of maternally deposited genes (DeLuca et al. 2020; McCarthy et al. 2022; Sarkar et al. 2023) The mechanism by which these large gene expression changes are regulated during this transition is not fully understood.

Changes in global genome organization play critical roles in regulating differentiation and gene expression (Spitz and Furlong 2012; Gonzalez-Sandoval and Gasser 2016; Misteli 2020; Dean et al. 2021; Galouzis and Furlong 2022; van Mierlo et al. 2023). The genome is partitioned into compartments mediated by the formation of conserved topologically associated domains (TADs) (Dekker et al. 2002; Ulianov et al. 2016; Sati and Cavalli 2017; Liao et al. 2021; Mohana et al. 2023). Each TAD contains genes and regulatory elements that interact more frequently with each other than with regions outside of the TAD (Dekker et al. 2002; Sati and Cavalli 2017; Szabo et al. 2018; Liao et al. 2021). TADs are demarcated by boundary elements that interact with insulator proteins, such as cohesin, CTCF, and BEAF, as well as various transcription factors (Yang et al. 2012; Nanni et al. 2020; Cavalheiro et al. 2023). TADs can regulate gene expression by facilitating enhancer–promoter interactions within their boundaries while insulating genes from neighboring regulatory elements (Burgess-Beusse et al. 2002; Yang and Corces 2011; Gonzalez-Sandoval and Gasser 2016; Sati and Cavalli 2017; Arzate-Mejía et al. 2020; Cavalheiro et al. 2021; Dean et al. 2021; Zuin et al. 2022). Lamin-associated domains (LADs) are TADs that are associated with the nuclear periphery (Briand and Collas 2020; Nazer 2022) and often contain genes that are transcriptionally silenced or exhibit low expression, which are marked by repressive chromatin marks, including methylated H3K9 (van Bemmel et al. 2010; Zullo et al. 2012; van Steensel and Belmont 2017). Early oogenesis genes such as *rpS19b* are silenced and tethered to the nuclear periphery, but how these genes are recruited to the nuclear periphery is not known.

The transcription factor Stonewall (Stwl) is required for *Drosophila* oogenesis (Clark and McKearin 1996; Brun et al. 2006; Maines et al. 2007; Zinshteyn and Barbash 2022), accumulates at insulator elements, and interacts with heterochromatin components such as HP1 (Brun et al. 2006; Maines et al. 2007; Zinshteyn and Barbash 2022). Intriguingly, loss of *stwl* phenocopies loss of *SETDB1* or *Nup*s, resulting in egg chambers that fail to grow, leading in sterility (Clark and McKearin 1996; Maines et al. 2007; Colozza et al. 2011; Clough et al. 2014; Zinshteyn and Barbash 2022; Sarkar et al. 2023). However, how Stwl regulates oogenesis was not fully known (Brun et al. 2006; Maines et al. 2007; Zinshteyn and Barbash 2022). Here, we discovered that *stwl*, like *SETDB1* and components of the NPC, represses early oogenesis genes during differentiation but is also critical for activating a cohort of maternally supplied genes. We show that Stwl coordinates gene expression changes at the GMT and promotes differentiation by stabilizing chromatin boundaries and promoting tethering of silenced genes to the nuclear periphery.

Results

Stwl is required during oocyte specification to silence reporters of rpS19b *and Blanks in the egg chambers*

As loss of *stwl* phenocopies loss of *SETDB1* (Clark and McKearin 1996; Brun et al. 2006; Zinshteyn and Barbash 2022; Sarkar et al. 2023), we hypothesized that *stwl* could regulate the expression of early oogenesis genes. To test this hypothesis, we generated control and *stwl* mutant flies carrying a reporter of *rpS19b*, *rpS19b::GFP*, which is under endogenous control (McCarthy et al. 2022). *stwl* mutant ovaries lose stem cells and contain egg chambers that do not grow, consistent with previous data (Supplemental Fig. S1A,B; Clark and McKearin 1996; Maines et al. 2007; Zinshteyn and Barbash 2022; Chavan et al. 2024). We stained ovaries of control and *stwl* mutants carrying the *rpS19b::GFP* for GFP and 1B1, which marks the somatic cell membranes, spectrosomes, and fusomes in the germline (Zaccai and Lipshitz 1996). We also independently stained control and *stwl* mutant ovaries for another early oogenesis protein, Blanks, along with 1B1 (Rust et al. 2020; Slaidina et al. 2020; Blatt et al. 2021). In contrast to control ovaries, where RpS19b::GFP and Blanks are silenced in the differentiated egg chambers, in *stwl* mutants, we found that RpS19b::GFP and Blanks are ectopically expressed in the egg chambers (Fig. 1B–G; Supplemental Fig. S1C). Thus, *stwl* is required for silencing both RpS19b::GFP and Blanks expression in the egg chambers.

Using an antibody raised against Stwl (Chavan et al. 2024), we found that Stwl is expressed in both the germline and the soma of the ovary (Supplemental Fig. S1D, D1). This expression is attenuated in *stwl* mutants (Supplemental Fig. S1E,E1,N). To determine whether germline expression of *stwl* is required to promote the silencing of early oogenesis genes, we used a germline-specific driver, *nanos(nos)GAL4*, to drive RNAi to deplete *stwl* in the germline of *RpS19b::GFP* reporter flies (Doren et al. 1998). Germline knockdown (GKD) of *stwl* resulted in egg chambers that do not grow (Supplemental Fig. S1A, B,F,F1,N) and in ectopic RpS19b::GFP and Blanks expression in egg chambers, similar to *stwl* mutants (Fig. 1H–K,G). Loss of *stwl* in the soma using a gonadal somatic cell-specific driver, *traffic jam(tj)GAL4*, does not result in a phenotype or upregulate Blanks in the egg chambers (Supplemental Fig. S1G,H; Li et al. 2003). From these data, we infer that Stwl is required in the germline to promote the silencing of RpS19b::GFP and Blanks in the egg chambers.

Stwl levels increase in the cyst stages of differentiation (Supplemental Fig. S1I,I1,N). Early oogenesis genes *rpS19b* and *blanks* are silenced starting in the cyst stages

mediated by SETDB1-dependent heterochromatin formation and then maintained in a silenced state in the egg chambers (Sarkar et al. 2023). To determine whether Stwl is required in the cyst stages during the initiation of silencing or in the later stages for the maintenance of the silenced state, we depleted *stwl* in the cyst stages using *bag of marbles(bam)GAL4* (Supplemental Fig. S1J,K,N) and in differentiated egg chambers using *MatαGAL4* (Januschke et al. 2002; Chen and McKearin 2003b). Compared with the control, we found that loss of *stwl* in cyst stages resulted in egg chambers that do not grow and express RpS19b::GFP and Blanks (Fig. 1L–P; Supplemental Fig. S1B; Chavan et al. 2024). In contrast, *stwl* depletion using *MatαGAL4* did not result in a phenotype or upregulation of RpS19b::GFP (Supplemental Fig. S1L,M). Taken together, we found that *stwl* is required during differentiation in cyst stages for egg chamber growth and for silencing RpS19b::GFP and Blanks.

Stwl is required to silence early oogenesis genes and activate a cohort of maternal genes

To determine whether *stwl* regulates other early oogenesis genes, we conducted RNA sequencing (RNA-seq) of whole control and *stwl* GKD ovaries immediately after eclosion (Blatt et al. 2021). Importantly, we analyzed both *nosGAL4*-mediated and *bamGAL4*-mediated GKD of *stwl* (Fig. 2A; Supplemental Table S1). We used a twofold cutoff (fold change of $-2 > (\log_2 FC) > 2$) and adjusted P-value < 0.05 to identify significantly dysregulated genes. The overlapping set of genes in the two GKD ovaries reports on Stwl-regulated genes in the cyst stages of the germline. We used this overlapping set of genes dysregulated in both *nosGAL4*-mediated and *bamGAL4*-mediated *stwl* depletion for all further analysis.

We found that 60% of the upregulated genes (1496 genes) are shared between *nosGAL4*-mediated and *bamGAL4*-mediated *stwl* GKD (Fig. 2B). Among these upregulated genes were *rpS19b* and *blanks*, consistent with our data showing that RpS19b::GFP and Blanks were ectopically expressed upon loss of *stwl* (Fig. 2A–C). We further validated that *rpS19b* RNA was upregulated in the *stwl* GKD egg chambers compared with the control by probing for its RNAs using in situ hybridization (Supplemental Fig. S2A–B1). To determine whether the other genes upregulated upon *stwl* GKD were early oogenesis genes, we plotted the abundance of the upregulated RNAs by using available RNA-seq libraries that were enriched for undifferentiated stages (GSCs and cystoblasts), differentiating stages when oocytes are specified (cysts), and differentiated stages (early egg chambers and late-stage egg chambers) (Fig. 2D; Blatt et al. 2021; McCarthy et al. 2022). We found that the upregulated genes are expressed in the undifferentiated stages and then are repressed in the differentiated stages in a Stwl-dependent manner (Fig. 2D). GO term analysis suggested that the genes upregulated upon loss of Stwl included cell differentiation genes, consistent with them being early oogenesis genes (Fig. 2E). Some Stwl-regulated early oogenesis genes were also SETDB1-regulated early oogenesis genes, as we found a 48% overlap of the upregulated genes, including *rpS19b* and *blanks* (Supplemental Fig. S2C; Sarkar et al. 2023). These data suggest that while Stwl and SETDB1 coregulate the expression of genes, they also independently regulate a large cohort of genes. Thus, *stwl* promotes the silencing of genes, including a cohort of SETDB1-regulated early oogenesis genes, at the onset of oocyte specification.

Additionally, we found that 40% of downregulated genes (370 genes) are shared between *nosGAL4*-mediated and *bamGAL4*-mediated *stwl* GKD (Fig. 2F). By plotting the abundance of the downregulated RNAs upon *stwl* GKD using available RNA-seq libraries that were enriched for different stages of oogenesis, we found that downregulated RNAs under control conditions are attenuated in the undifferentiated stages and are then expressed in the differentiated stages in an Stwl-dependent manner (Fig. 2G; McCarthy et al. 2022). The GO term analysis of the downregulated genes suggested that the genes are involved in egg activation, meiosis I, and the nucleosome assembly process, consistent with a failure in oogenesis and sterility upon loss of *stwl* (Fig. 2H). Downregulated genes included maternally deposited genes such as *polar granule component* (*pgc*) and *wispy* (*wisp*) (Supplemental Fig. S2D; Nakamura et al. 1996; Cui et al. 2008; Rangan et al. 2009). We validated that *pgc* RNA was downregulated in the *stwl* GKD egg chambers compared with the control by probing for its RNAs using in situ hybridization (Supplemental Fig. S2E–F1). However, other maternally provided RNAs, such as *hunchback*, were not downregulated (Supplemental Fig. S2G; Wharton and Struhl 1991; Tautz and Nigro 1998). Thus, Stwl is required to upregulate a cohort of genes that are critical to promote oogenesis, fertility, and embryonic development.

Stwl binds at promoters and overlaps with boundary element proteins but does not directly regulate a large fraction of upregulated genes

To determine whether Stwl regulates its targets directly, we conducted cleavage under targets and release using nuclease (CUT&RUN) using the Stwl antibody (Skene and Henikoff 2017; Ahmad and Spens 2019). We probed Stwl binding in the early stages of oogenesis in *bam* GKD ovaries, which are enriched for undifferentiated stages, and adult wild-type ovaries, which are enriched for differentiated egg chambers (Chen and McKearin 2003a,b). We used *stwl* GKD ovaries and IgG as negative controls (Fig. 3A). We found that Stwl binding to the genome increases from undifferentiated (CBs) to differentiated (egg chambers) stages, consistent with the antibody staining showing an increase in Stwl levels in the cyst stages (Supplemental Fig. S1I,I1,N). The association of Stwl with the genome is reduced upon *stwl* GKD and is absent in the IgG-only sample (Fig. 3A). Taken together, we found that the Stwl binding signal from CUT&RUN during oogenesis is specific.

In the differentiated egg chambers, Stwl was mostly bound at promoters and, to a lesser extent, in intergenic regions and introns (Fig. 3B). We performed motif enrichment analysis and found regions, including a TATCGATAGC motif, to be enriched (Fig. 3C). The enrichment

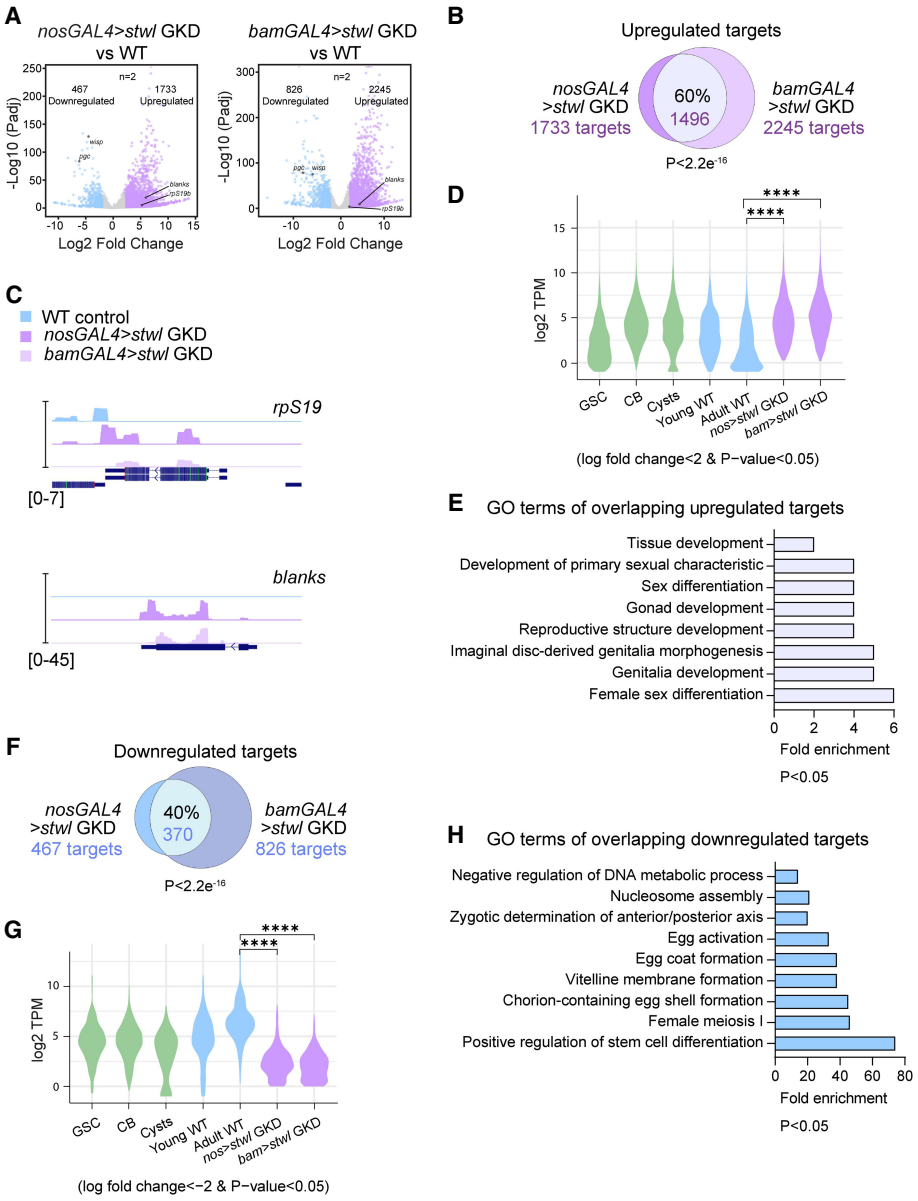

Figure 2. Stwl regulates the silencing of early oogenesis genes and activation of some maternal genes. (*A*) Volcano plots of $-\log_{10}$ *P*-value versus $\log_2$fold change (FC) of *nosGAL4>stwl* GKD ovaries versus *nosGAL4* (control) ovaries as well as *bamGAL4>stwl* GKD ovaries versus *bamGAL4* (cyst control) ovaries showing significantly downregulated (blue) and upregulated (lilac) transcripts in *stwl* GKD ovaries compared with control ovaries. Adjusted *P*-value < 0.05; genes with twofold or higher change were considered significant. $n = 2$. (*B*) Venn diagram of upregulated genes from RNA-seq of *nosGAL4>stwl* GKD ovaries and *bamGAL4>stwl* GKD ovaries compared with controls. Sixty percent of targets are shared between both. Statistics were derived from hypergeometric tests. $P < 2.2 \times 10^{-16}$. (*C*) RNA-seq tracks showing that *rpS19b* and *blanks* are upregulated upon *stwl* GKD (*nosGAL4*; dark purple) and in the cyst stages (*bamGAL4*; light purple) compared with control (blue). (*D*) Violin plot of RNA levels of the shared upregulated targets (*nosGAL4>stwl* GKD and *bamGAL4>stwl* GKD) in ovaries enriched for GSCs, cystoblasts, and cysts and in whole ovaries, showing that Stwl upregulated targets are expressed up to the cyst stages and attenuated in whole ovaries. Statistics were derived from a negative binomial regression model that was used to estimate the average TPM count of "signature" genes between each "genotype." The TPM of each gene was used as the dependent variable, and "genotype" was the independent variable. Statistical comparisons between groups were performed using contrasts, and *P*-values were adjusted for multiple comparisons using the Benjamini–Hochberg procedure false discovery rate (*P*-FDR). The average TPM between groups was considered to be significantly different when *P*-FDR < 0.05. (*E*) The biological process GO terms of shared upregulated genes in *nosGAL4>stwl* GKD and *bamGAL4>stwl* GKD ovaries compared with controls using fold enrichment. Statistics were derived from Fisher's exact tests. Results are displayed for FDR < 0.05. (*F*) Venn diagram of downregulated genes from RNA-seq of *nosGAL4>stwl* GKD and *bamGAL4>stwl* GKD ovaries compared with controls. Forty percent of targets are shared between both. Statistics were derived from hypergeometric tests. $P < 2.2 \times 10^{-16}$. (*G*) Violin plot of RNA levels of the shared downregulated targets (*nosGAL4>stwl* GKD and *bamGAL4>stwl* GKD) in ovaries enriched for GSCs, cystoblasts, and cysts and in whole ovaries, showing that Stwl downregulated targets are expressed at higher levels in the differentiated stages. Statistics were derived from a negative binomial regression model that was used to estimate the average TPM count of "signature" genes between each "genotype." The TPM of each gene was used as the dependent variable, and "genotype" was the independent variable. Statistical comparisons between groups were performed using contrasts, and *P*-values were adjusted for multiple comparisons using the Benjamini–Hochberg procedure (*P*-FDR). The average TPM between groups was considered to be significantly different when *P*-FDR < 0.05. (*H*) The biological process GO terms of shared downregulated genes in *nosGAL4>stwl* GKD and *bamGAL4>stwl* GKD ovaries compared with controls using fold enrichment. Statistics were derived from Fisher's exact tests. Results are displayed for FDR < 0.05.

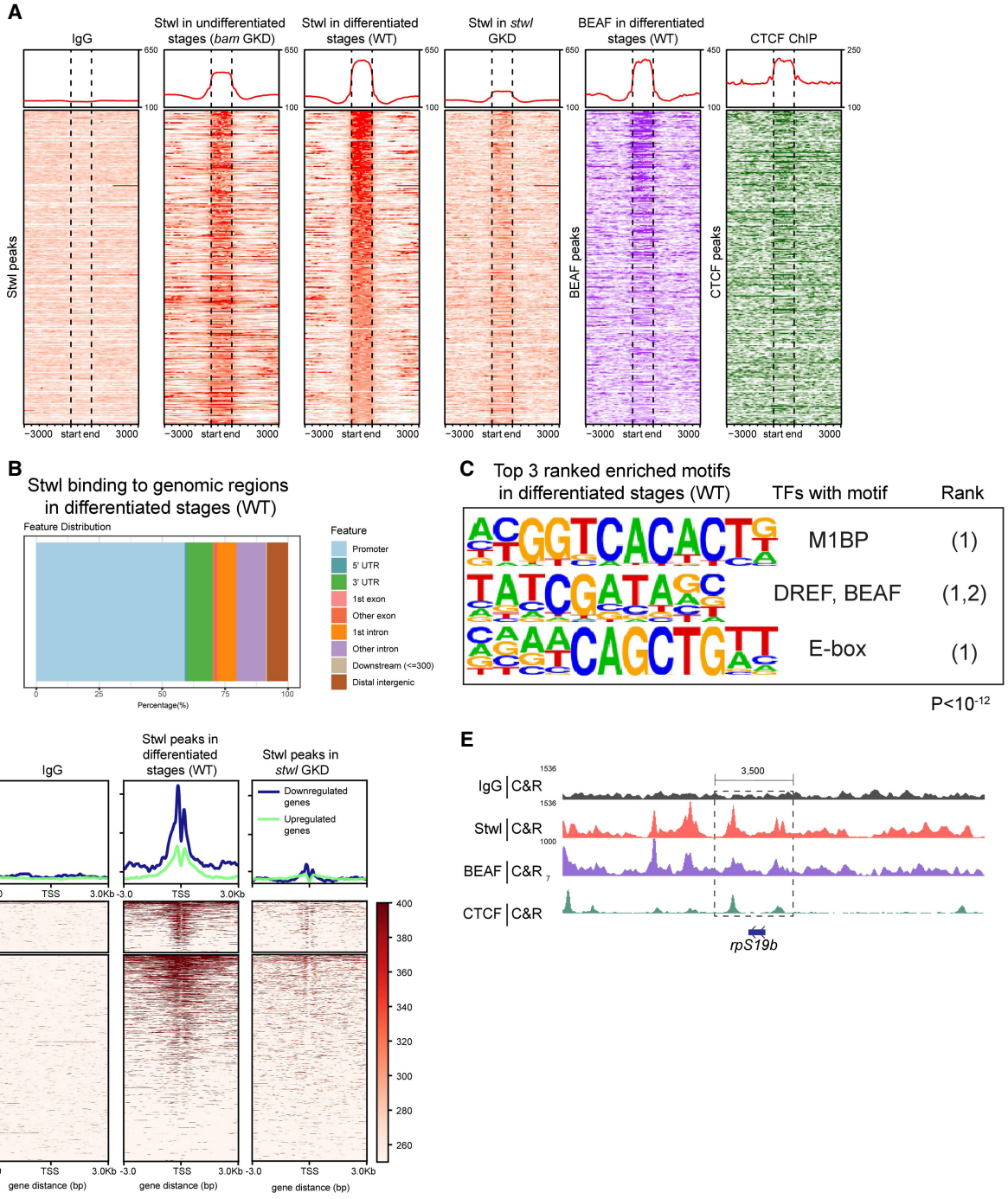

Figure 3. Stwl binds proximal to promoters and overlaps with boundary element proteins but does not directly regulate a large fraction of the dysregulated genes. (*A*) CUT&RUN occupancy of IgG peaks in ovaries (negative control), Stwl peaks in undifferentiated stages, Stwl peaks in differentiated stages (8585 peaks), Stwl peaks upon *stwl* GKD, BEAF peaks in WT differentiated stages (WT ovaries; shown in purple), and CTCF ChIP-seq peaks in the larval CNS (shown in green). Heat maps showing −3 kb and +3 kb around the start and end of Stwl peaks (shown in red). Black dashed lines represent the start and end of Stwl peaks. These heat maps show an overlap between Stwl, BEAF, and CTCF binding. (*B*) Graph showing percentages of Stwl binding pattern to genomic regions in the differentiated stages. This shows that Stwl binds mainly to promoters (60%). (*C*) HOMER motif analysis of Stwl binding sites in the differentiated stages showing the top three ranked motifs also bound by other transcription factors: M1BP, DREF/BEAF, and E-box-associated. $P < 10^{-12}$. (*D*) CUT&RUN occupancy of IgG peaks in WT ovaries (negative control), Stwl peaks in differentiated stages (WT ovaries), and Stwl in *Stwl* GKD for RNA-seq upregulated and downregulated targets. Heat maps showing −3 kb and +3 kb around the TSSs of target genes. These heat maps show that Stwl, BEAF, and CTCF bind a portion of downregulated and upregulated targets. (*E*) CUT&RUN occupancy track for the *rpS19b* locus for IgG (negative control; gray), Stwl peaks in differentiated stages of WT ovaries (red), BEAF peaks in differentiated stages of WT ovaries (purple), and CTCF ChIP-seq (green) showing Stwl, BEAF, and CTCF flanking the *rpS19b* locus from both sides.

of this motif, which is bound by proteins such as boundary element-associated factor-32 (BEAF-32), is consistent with previous observations from ChIP-seq carried out for Stwl in S2 cells (Fig. 3C; Zinshteyn and Barbash 2022). BEAF is an insulator protein that binds to boundary elements to regulate genome organization and chromatin state (Yang et al. 2012; Van Bortle et al. 2014; Avva and Hart 2016). To determine whether Stwl is associated with boundary elements during oogenesis, we carried out CUT&RUN for BEAF and also used published ChIP-seq data for another boundary element protein, CCCTC-binding factor (CTCF) (Fig. 3A; Kaushal et al. 2021). We found that Stwl binding regions partially overlapped with regions bound by BEAF and CTCF (Supplemental Fig. S3A–C). The overlap of Stwl binding peaks was more with BEAF than with CTCF (Supplemental Fig. S3C). Thus, Stwl is associated with promoter regions of the genome and overlaps with the insulator proteins BEAF and CTCF.

To determine whether Stwl directly regulates early oogenesis genes, we integrated our RNA-seq and CUT&RUN data from control and *stwl* GKD ovaries. We found that in the differentiated stages, Stwl binds 23% of the upregulated targets and 44% of the downregulated targets above the baseline signal (Fig. 3D). Some upregulated early oogenesis genes, such as *rpS19b*, have Stwl binding sites, while others, such as *blanks*, do not have any clear Stwl binding site proximal to the transcriptional start sites (TSSs) (Fig. 3E; Supplemental Fig. S3B). These data suggest that Stwl binds proximal to a cohort of both upregulated and downregulated targets but does not directly regulate a large cohort of upregulated genes.

Stwl regulates early oogenesis genes by recruiting BEAF

As Stwl and BEAF binding sites overlap (Supplemental Fig. S3C), we wondered whether Stwl exerts its activity via recruiting insulator protein BEAF (Roy et al. 2007; Avva and Hart 2016). If Stwl recruits BEAF to regulate gene expression, we predicted that (1) loss of *BEAF* would phenocopy loss of *stwl*, (2) BEAF and Stwl would coregulate a subset of genes, and (3) loss of *stwl* would result in loss of BEAF at various genomic locations.

Using previously characterized *BEAF* mutants, we stained ovaries of control and *BEAF* mutants with Vasa and 1B1 (Lasko and Ashburner 1988; Zaccai and Lipshitz 1996; Avva and Hart 2016). We found that *BEAF* mutants are sterile, with ovarioles containing egg chambers that do not grow (100%, $n = 50$ ovarioles), like *stwl* mutants (Supplemental Fig. S3D,E; Roy et al. 2007). To next determine whether *BEAF* and *stwl* both coregulate early oogenesis genes, we conducted RNA-seq of control and *BEAF* mutant ovaries. We found that 60% of the upregulated genes are shared upon loss of *BEAF* and *stwl* (Supplemental Fig. S3F,G). Among these upregulated genes was *rpS19b* (Supplemental Table S1).

Through antibody staining, we found that, like Stwl, BEAF expression was attenuated in the undifferentiated cells and increased as the cysts differentiated into oocytes (Supplemental Fig. S3H,I; Hart et al. 1999; Pathak et al. 2021). In addition, we found that Stwl is present in the nucleus upon loss of *BEAF* (Supplemental Fig. S3J–K1). By carrying out CUT&RUN, we found that loss of *stwl* results in loss of BEAF binding at various genomic locations (Supplemental Fig. S3L). However, not all of BEAF's genomic binding is subject to regulation by Stwl. We found that a subset of BEAF also binds to genomic sites independently of Stwl (Supplemental Fig. S3L). These data suggest that Stwl recruits BEAF to a cohort of genomic loci to regulate gene expression during oogenesis.

Stwl is required to demarcate active and silenced genomic compartments during differentiation

Stwl exhibits distinct binding patterns: It binds at promoters of select upregulated targets and downregulated targets. This observation hints at a more intricate mechanism for how Stwl regulates gene expression beyond merely binding to targets and promoting their silencing. Furthermore, we found that Stwl's binding overlaps with insulator proteins BEAF and CTCF, which can demarcate genomic boundaries, including TADs (Nanni et al. 2020; Cavalheiro et al. 2021; Herman et al. 2022). In addition, loss of *BEAF* partially phenocopies loss of *stwl*, and they coregulate silencing of a cohort of early oogenesis genes. Based on these data, we hypothesized that Stwl may influence gene expression by influencing genomic boundaries during differentiation. To test this hypothesis, we first probed Stwl's binding patterns and its relationship with the chromatin state and genomic organization before and after differentiation.

TADs can exhibit remarkable conservation across different cell types (Rao et al. 2014; Rowley et al. 2017). To determine where Stwl binds in relation to genome organization, we analyzed previously annotated TADs from salivary gland cells and Kc cells to determine the binding sites of Stwl, CTCF, and BEAF in the context of genomic organization (Eagen et al. 2015; Stadler et al. 2017; Ramírez et al. 2018). We also conducted a comprehensive analysis of the chromatin state on control gonads by examining H3K4me3 (associated with active promoters), H3K27ac and H3K4me1 (associated with active enhancers), H3K36me3 (associated with transcribed gene bodies), and H3K27me3 and H3K9me3 (associated with gene silencing) chromatin marks using CUT&RUN before and after differentiation (Bannister and Kouzarides 2011; Lawrence et al. 2016; Gates et al. 2017; Talbert and Henikoff 2021). We used these chromatin marks to build a seven state chromatin model (Supplemental Fig. S4A) and correlated TADs, Stwl/CTCF/BEAF binding sites, and the observed chromatin states (Ernst and Kellis 2017). By exploring these interconnections, we aimed to gain a better understanding of the role of Stwl in regulating the overall genome architecture and chromatin landscape.

Upon analysis of salivary gland and Kc cell TADs, we found the average length of salivary gland TADs to be much larger than Kc TADs, and the number of salivary gland TADs to be fewer than Kc TADs (Eagen et al. 2015; Stadler et al. 2017). In addition, we also found that all Kc TADs are encompassed within one or more salivary gland TADs. These data suggested that Kc cell TADs have

a higher resolution than salivary glands. Thus, we used Kc cell TADs for further analyses throughout the study (Supplemental Fig. S4B).

In control ovarioles enriched for differentiated egg chambers, we found that Stwl, BEAF, and CTCF bound to regions flanking the regions annotated as TADs in Kc cells (Fig. 4A). Stwl binding at the TAD boundaries increased from undifferentiated cells to differentiated egg chambers (Fig. 4A). *stwl* GKD results in loss of Stwl at these boundaries (Fig. 4A). In addition, we found that loss of *stwl* results in loss of BEAF at the boundaries (Fig. 4A). Thus, Stwl, CTCF, and BEAF are present at TAD boundaries, and Stwl recruits BEAF to these boundaries.

We next examined the chromatin state of these compartments in the undifferentiated and differentiated stages and *stwl* GKD. We found that in both the undifferentiated cells and differentiated egg chambers, Stwl binds at TAD boundaries and demarcates active chromatin (e.g., TSSs and enhancers) flanking the TADs from the quiescent genes present within the TADs (Fig. 4B). The increase in Stwl at these boundaries during differentiation coincided with changes to the chromatin state for both regions flanking and inside the TADs (Fig. 4B–D). For example, there was an increase in promoter activity (H3K4me3) in regions flanking the TADs during differentiation (Fig. 4C). There was also an increase in enhancer activity (H3K27ac), mostly at TADs boundaries and, at lower levels, within TADs in the differentiated stages (Fig. 4D). Overall levels of H3K27me3 within TADs did not appreciably change during differentiation (Fig. 4E). The changes associated with promoter and enhancer activity did not happen upon loss of *stwl* (Fig. 4A–D). Thus, during differentiation, the binding of Stwl, BEAF, and CTCF demarcates active and silenced chromatin in TADs, which influences the chromatin state at TAD boundaries and within TADs.

Stwl regulates the enhancer landscape to promote proper gene expression during differentiation

To determine how Stwl specifically affects gene expression, we examined the overlap between differentially expressed genes, TADs, and chromatin states in undifferentiated and differentiated controls as well as *stwl* GKD gonads. We found that most of the upregulated genes (63%) and downregulated genes (56%) are encompassed within TADs (Fig. 5A). To determine how Stwl regulates upregulated and downregulated genes, we analyzed the chromatin state of these genes separately.

Through analysis of genes that are downregulated upon *stwl* GKD, we found an increase in active marks at the TSS and a decrease in quiescence, consistent with these genes being activated at this stage (Fig. 5B; Supplemental Fig. S5A). However, upon *stwl* GKD, this increase in active marks does not occur at the promoters of the downregulated genes, and these genes remain quiescent (Fig. 5B). The principal component analysis (PCA) plot shows that active marks such as H3K4me3 and H3K27ac are dysregulated in *stwl* GKD compared with differentiated controls. The chromatin state of the promoters of the downregulated genes upon *stwl* GKD is closer to the undifferentiated stages than the differentiated stages (Supplemental Fig. S5B). For example, *pgc* and *wispy*, which are downregulated genes, show an increase in active marks during differentiation and a decrease in quiescence. The decrease in quiescence and increase in the active marks is attenuated upon *stwl* GKD (Supplemental Fig. S5C). Thus, Stwl contributes to expression of a cohort of maternal genes by promoting the acquisition of active histone marks during differentiation.

Analyzing the chromatin state of the upregulated genes upon *stwl* GKD, we observed changes in the enhancer landscape (Fig. 5C; Supplemental Fig. S5D). In control ovaries, in the undifferentiated stages, genomic regions encompassing upregulated genes are enriched for active enhancers, consistent with the fact that these genes are normally expressed at higher levels in the undifferentiated stages (Figs. 2D, 5C). During differentiation, we found that the levels of active enhancers decrease with an increase in "weak" enhancers, which are usually associated with inactive or poised genes, concomitant with these genes being silenced (Figs. 2D, 5C). Weak enhancers are defined as regions containing high levels of H3K4me1 and low levels of H3K27ac. In contrast, enhancers are defined by high levels of both H3K27ac and H3K4me1 (Supplemental Fig. S4A). These changes in "active" and "weak" enhancers during differentiation did not happen upon loss of *stwl*, and these genes continued to be expressed (Figs. 2D, 5C, D). The enhancer profile of *stwl* GKD resembles the enhancer profile of undifferentiated cells (Fig. 5C). Indeed, the PCA plot of histone marks of upregulated genes shows that enhancer marks (H3K27ac) are dysregulated in *stwl* GKD compared with differentiated controls (Supplemental Fig. S5E). For example, the genomic region proximal to *rpS19b* showed a decrease in active enhancers and an increase in weak enhancers during differentiation (Supplemental Fig. S5F). As Stwl and BEAF regulate a cohort of upregulated targets, we mapped BEAF binding sites to the upregulated targets and found that BEAF binding sites flank these targets, suggesting that Stwl could exert its enhancer activity through recruiting BEAF (Fig. 5C). Taken together, we infer that Stwl promotes silencing of a cohort of early oogenesis genes, such as *rpS19b*, during differentiation by regulating their promoter and their associated enhancers.

We previously found that SETDB1 regulates a subset of early oogenesis genes through promoting heterochromatin formation on their gene body (Sarkar et al. 2023). To ascertain whether Stwl directly regulates heterochromatin, we conducted an analysis of heterochromatic H3K9me3 domains following *stwl* GKD. We integrated RNA-seq data with H3K9me3 analysis to explore potential correlations between the upregulation of target genes upon *stwl* depletion and changes in H3K9me3 levels. We found that Stwl coregulates 48% of the upregulated genes in conjunction with SETDB1 (Supplemental Table S1). Of these coregulated genes, we observed a decrease in H3K9me3 levels on the gene body of 128 early oogenesis genes (11%) following *stwl* depletion (Supplemental Fig. S5G). Principal component analysis of all the coregulated genes suggests

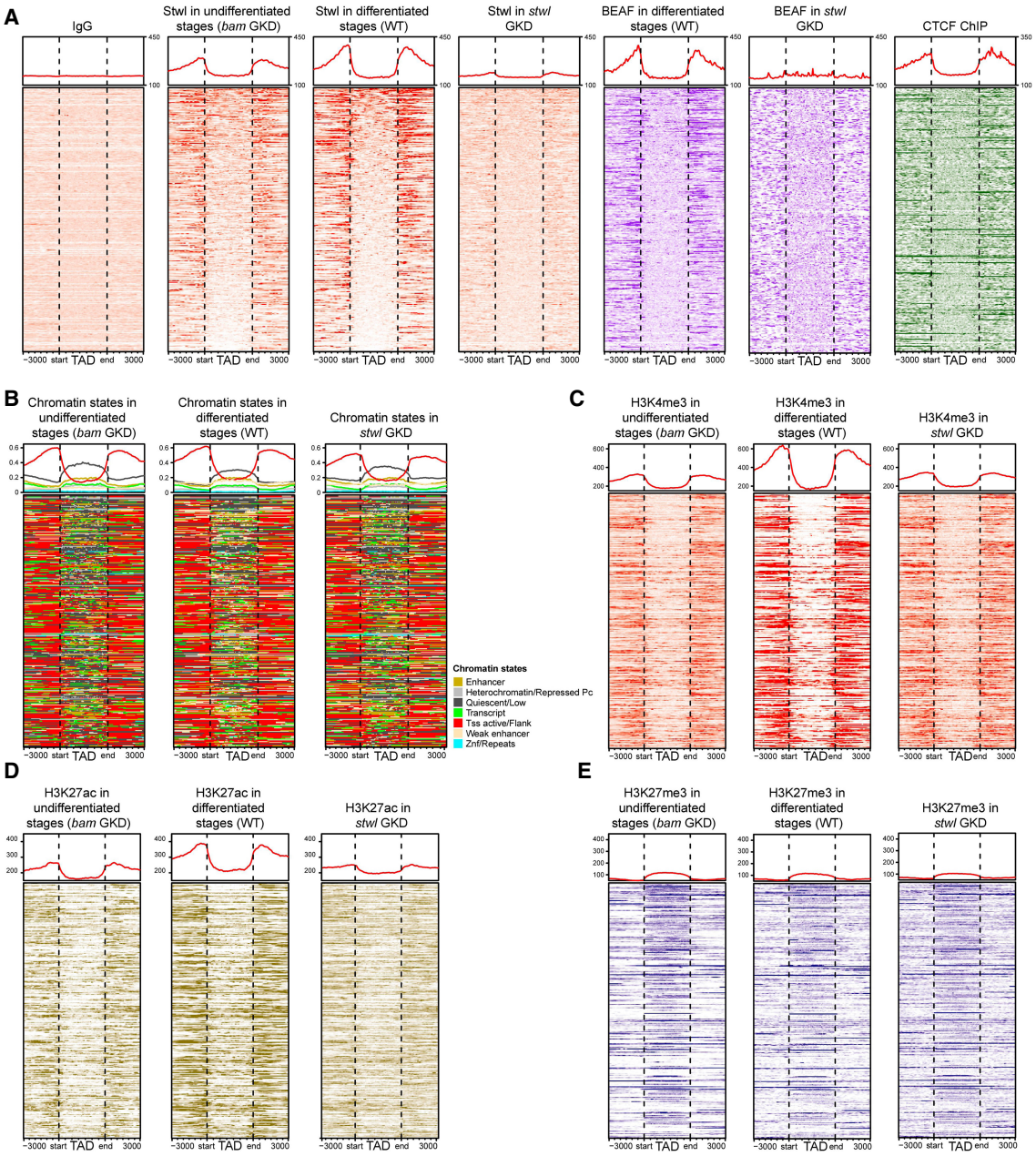

Figure 4. Stwl demarcates active and silenced genomic compartments during differentiation and is required for proper chromatin state. (*A*) CUT&RUN occupancy of IgG peaks in WT ovaries (negative control), Stwl peaks in undifferentiated stages (*bam* GKD), Stwl peaks in differentiated stages of WT ovaries, Stwl peaks in *stwl* GKD, and BEAF peaks in differentiated stages of WT ovaries in *stwl* GKD and CTCF. Occupancy heat maps are shown for TADs as well as −3 kb and +3 kb around the start and end of TADs. Black dashed lines represent the start and end of TADs. The heat maps show the binding of Stwl, BEAF, and CTCF at the boundaries of TADS. (*B*) Comprehensive analysis of seven chromatin states of undifferentiated stages (*bam* GKD), differentiated stages (WT ovaries), and *stwl* GKD ovaries built using multiple histone marks is shown for TADs. Heat map showing TADs as well as −3 kb and +3 kb around the start and end of TADs. Black dashed lines represent the start and end of TADs. Different states are indicated by color. (Gold) Enhancer, (light gray) heterochromatin/repressed, (dark gray) quiescent/low, (green) transcript, (red) TSS active/flank, (beige) weak enhancer, (blue) Znf/repeats. This seven state model shows Stwl demarcating active compartments at TAD boundaries and repressed compartments in TADs. (*C*) Heat maps of H3K4me3 active histone marks in undifferentiated stages (*bam* GKD), differentiated stages (WT ovaries), and *stwl* GKD ovaries are shown for TADs. Heat map showing TADS as well as −3 kb and +3 kb around the start and end of TADs. Black dashed lines represent the start and end of TADs. Heat maps showing that the H3K4me3 histone mark profile of *stwl* GKD resembles that of undifferentiated stages. (*D*) Heat maps of the H3K27ac active enhancer histone mark in undifferentiated stages (*bam* GKD), differentiated stages (WT ovaries), and *stwl* GKD ovaries are shown for TADs. Heat map showing TADS as well as −3 kb and +3 kb around the start and end of TADs. Black dashed lines represent the start and end of TADs. Heat maps showing that the H3K27ac histone mark profile of *stwl* GKD resembles that of undifferentiated stages. (*E*) Heat maps of the H3K27me3 repressive histone mark in undifferentiated stages (*bam* GKD), differentiated stages (WT ovaries), and *stwl* GKD ovaries are shown for TADs. Heat map showing TADs as well as −3 kb and +3 kb around the start and end of TADs. Black dashed lines represent the start and end of TADs. Heat maps showing that the H3K27me3 histone mark profile of *stwl* GKD resembles that of undifferentiated stages as well as differentiated stages.

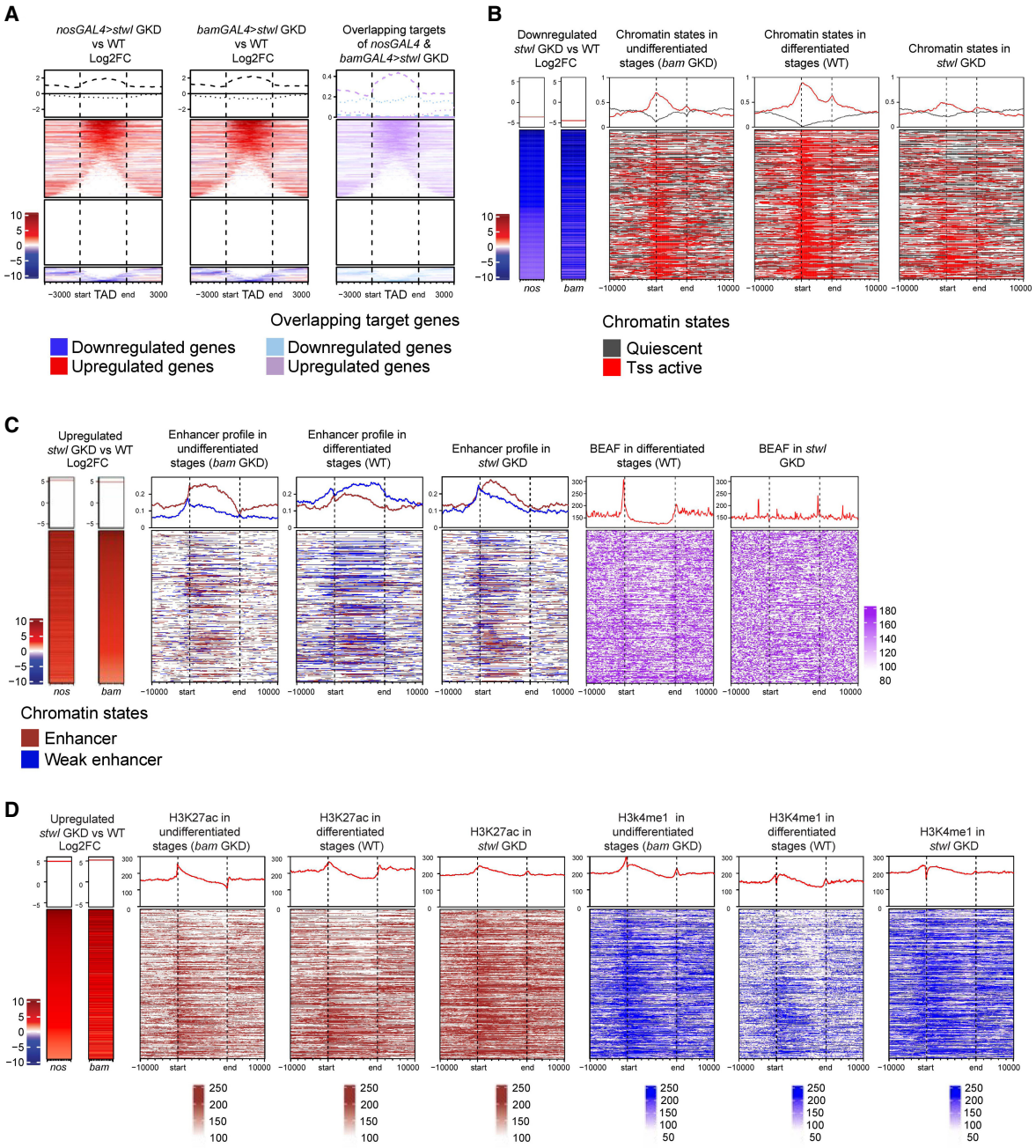

Figure 5. Stwl regulates enhancers to promote gene expression. (*A*) Heat maps of lfc2 sorted for RNA-seq Stwl targets at TADs. Upregulated targets are shown in red, and downregulated targets are shown in blue. Overlapping targets shared between *nosGAL4>stwl* GKD and *bamGAL4>stwl* GKD showing upregulated targets in TADs (lilac) and downregulated targets (blue). Heat maps are shown for TADS as well as −3 kb and +3 kb around the start and end of TADs. Black dashed lines represent the start and end of TADs. The heat maps are divided into three clusters: the upregulated target cluster, the nontarget gene cluster, and the downregulated target cluster. The heat maps show that both genes upregulated upon *stwl* GKD and genes downregulated upon *stwl* GKD are present within TADs. (*B*) Heat maps of lfc2 sorted for RNA-seq Stwl downregulated targets in *stwl* GKD (blue). Heat maps show chromatin states for those targets in undifferentiated stages (*bam* GKD), differentiated stages of wild-type ovaries, and *stwl* GKD ovaries. Different states are indicated by color ([dark gray] quiescent/low, [red] TSS active/flank), showing an increase in active marks at the TSSs of genes and a decrease of quiescence during differentiation. These changes in chromatin states do not occur upon *stwl* GKD. (*C*) Heat maps of lfc2 sorted for RNA-seq Stwl upregulated targets in *stwl* GKD (red). Heat maps show enhancer states for those targets in undifferentiated stages (*bam* GKD) and differentiated stages of wild-type ovaries. Enhancer profile heat maps are shown for upregulated targets in undifferentiated stages (*bam* GKD), differentiated stages of wild-type ovaries, and *stwl* GKD ovaries showing changes in enhancer profiles during differentiation that do not occur upon *stwl* GKD. BEAF binding sites are mapped at Stwl upregulated targets in *stwl* GKD. (*D*) Heat maps of lfc2 sorted for RNA-seq Stwl upregulated targets in *stwl* GKD (red). Heat maps show enhancer state markers (H3K27ac and H3K4me1) for those targets in undifferentiated stages (*bam* GKD) and differentiated stages of WT ovaries. Enhancer profile marker heat maps are shown for upregulated targets in undifferentiated stages (*bam* GKD), differentiated stages of WT ovaries, and *stwl* GKD ovaries showing changes in enhancer profile markers during differentiation that do not occur upon *stwl* GKD.

that Stwl regulates most of these shared targets with SETDB1 at the level of enhancers rather than through the regulation of heterochromatin deposition on the gene body (Supplemental Fig. S5H). However, we cannot exclude the possibility that SETDB1 deposits heterochromatin on distal enhancer of these upregulated genes. Thus, Stwl primarily exerts its influence mostly via enhancers rather than by directly regulating heterochromatin formation on the gene body.

Stwl promotes the expression of nucleoporins and, consequently, NPC formation

We were interested in understanding how Stwl, which is present at TAD boundaries, contributes to changes to the expression of genes inside TADs. NPCs can help position chromatin domains to the nuclear lamina to maintain their silenced state (Strambio-De-Castillia et al. 2010; Bank and Gruenbaum 2011; Ibarra and Hetzer 2015; van Steensel and Belmont 2017; Briand and Collas 2020; Nazer 2022). We previously described a role for NPCs in maintaining the silencing of early oogenesis genes such as *rpS19b* by tethering them to the nuclear periphery (Sarkar et al. 2023). Intriguingly, loss of individual Nups in the germline phenocopies loss of *stwl* (Colozza et al. 2011; Sarkar et al. 2023). Building on these findings, we asked whether Stwl affects the expression of Nups.

From visual inspection of downregulated targets, we observed a significant decrease in the expression levels of four nucleoporins (Nups), which were downregulated by more than twofold upon the loss of *stwl* (Fig. 6A; Supplemental Table S1). Another 10 were also downregulated but did not meet the twofold cutoff. These downregulated Nups did not belong to a specific NPC subcomplex. Instead, we discovered that these Nup genomic loci were bound by Stwl and BEAF around the TSS (Fig. 6A). For example, for the Nup *aladin*, which is downregulated upon the loss of *stwl*, there is a decrease of quiescence in the genomic region proximal to it during differentiation. This change in quiescence did not occur upon *stwl* GKD (Supplemental Fig. S6A; Nallasivan et al. 2021). Taken together, we found that Stwl promotes the expression of a specific cohort of Nups by creating a barrier between active and repressed chromatin regions during differentiation.

Considering that all Nups are required to form functional NPCs, we hypothesized that the loss of *stwl* would disrupt NPC assembly. To test this hypothesis, we examined NPC formation in control and *stwl* GKD conditions using the mAb414 antibody, a marker for NPCs (Davis and Blobel 1987; Capelson et al. 2010a; Yang and Corces 2011; Sarkar et al. 2023). From immunostaining, we found that NPC levels did not increase in the nurse cells of the egg chambers in *stwl* GKD ovaries like they did in the controls (Fig. 6B–D). We used nurse cells for quantitation, as *stwl* mutants do not properly specify an oocyte (Clark and McKearin 1996). In addition, when there was NPC staining present in *stwl* GKD ovaries, we found that there were gaps in the distribution of NPCs in the nuclear membrane (Supplemental Fig. S6B–C1). Thus, Stwl is required for proper NPC formation.

Stwl and NPCs promote tethering of silenced genes to the nuclear lamina

Chavan et al. (2024) have shown that Stwl physically interacts with components of the NPC. We hypothesized that Stwl not only promotes NPC formation but, via interaction with NPCs, can promote the association of chromatin compartments to the nuclear periphery (Bank and Gruenbaum 2011; Ulianov et al. 2019; Briand and Collas 2020; Chavan et al. 2024). To test this hypothesis, we first asked whether Stwl and NPCs colocalize at the nuclear periphery. By staining for NPCs and Stwl, we found that Stwl and NPCs indeed colocalize (Supplemental Fig. S7A–B2). Given that Stwl is observed at TAD boundaries and interacts with NPCs. We hypothesized that NPCs might also be present at these TAD boundaries. To test this, we analyzed Nup binding sites in the genome using available ChIP-seq data for Nup 107 and Elys from Kc cells. (Gozalo et al. 2020). We found that the NPC components Elys and Nup107 were present flanking TAD boundaries (Supplemental Fig. S7C). These observations suggest that Stwl and NPC members interact and are present at TAD boundaries.

We next wished to determine whether Stwl plays a role in tethering TADs to the nuclear lamina to promote LAD formation and contribute to gene silencing (Ciabrelli and Cavalli 2015; Czapiewski et al. 2016; Szabo et al. 2018). To determine this, we overlapped published LADs, Lamin binding sites, and nucleoporin Elys binding sites with the data we generated of chromatin state, Stwl binding sites, and upregulated targets of Stwl (Ciabrelli and Cavalli 2015; Czapiewski et al. 2016; Szabo et al. 2018).

We found that, consistent with previous findings, most LADs are also transcriptionally inactive during oogenesis (Fig. 7A). We found that 36% of genes upregulated upon Stwl depletion are located within LADs (Fig. 7A). Furthermore, we found that Stwl binding sites overlapped with Lamin C binding sites, LAD boundaries (Fig. 7A; Ulianov et al. 2019). Additionally, we also observed the presence of Stwl, BEAF, and NPC member Elys binding at the periphery of LADs (Fig. 7A). These findings suggest an interaction between Stwl and NPCs, facilitating the association of LADs with the nuclear lamina. We examined the genomic position of the early oogenesis gene *blanks* and found that not only were the TAD boundaries associated with Lamin C, but the *blanks* locus itself was also associated with Lamin C (Supplemental Fig. S7D). We also found that the early oogenesis gene *rpS19b* is not part of a TAD/LAD and that Stwl binding sites that flank this locus overlap with Lamin C (Supplemental Fig. S7D).

Previously, we observed that depletion of *nup154* in the germline leads to the detachment of the *rps19b* locus from the nuclear periphery, accompanied by upregulation of *rps19b* expression (Sarkar et al. 2023). To further investigate whether Stwl facilitates the tethering of silenced genes to the nuclear lamina, we conducted DNA fluorescent in situ hybridization (FISH) using probes specific to the *rpS19b* locus in control, *stwl* GKD, and *BEAF* mutant ovaries (Sarkar et al. 2023). In control ovarioles, we consistently observed the *rpS19b* locus positioned at the nuclear

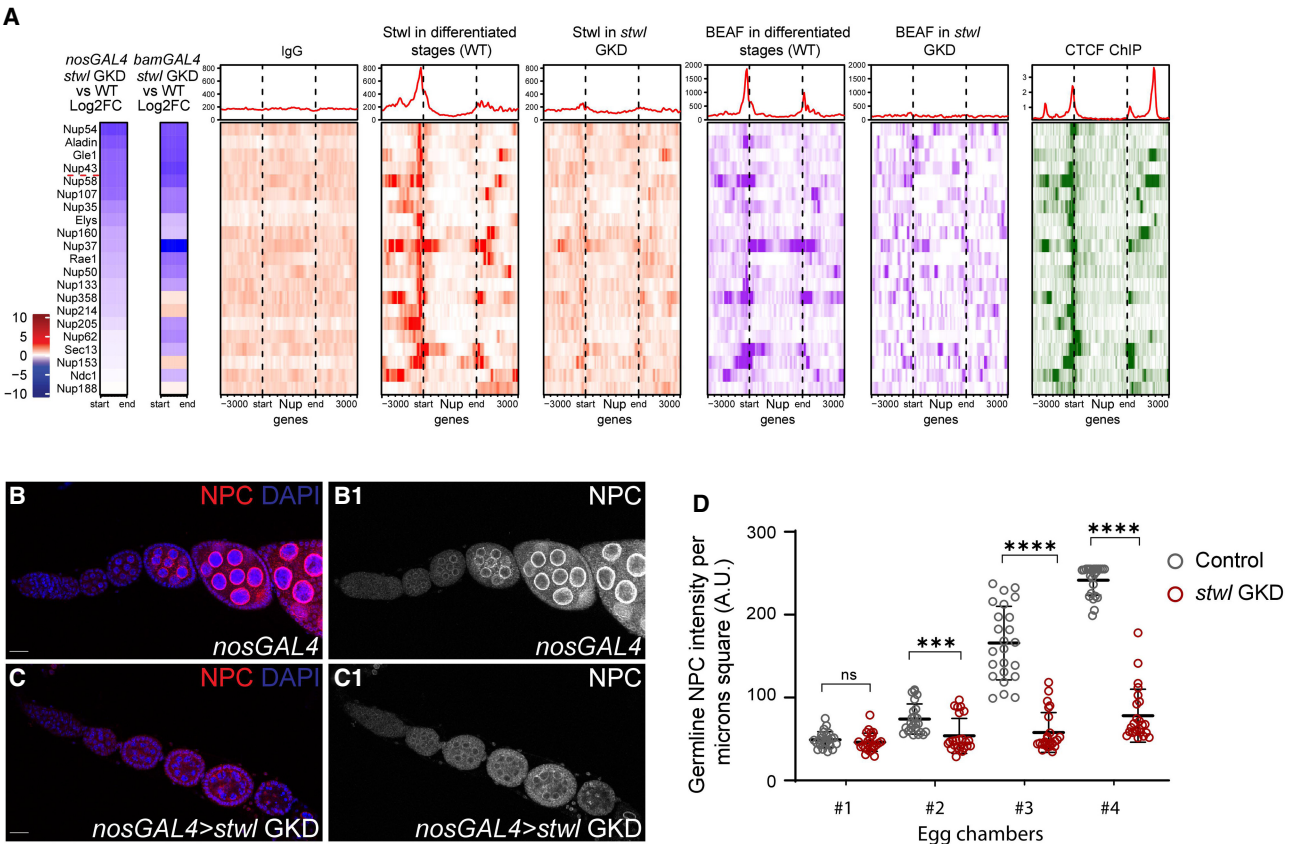

Figure 6. Stwl promotes the expression of nucleoporins to promote NPC formation. (*A*) CUT&RUN occupancy of IgG peaks in WT ovaries (negative control), Stwl peaks in undifferentiated stages of ovaries, Stwl peaks in differentiated stages of WT ovaries, Stwl peaks upon *stwl* GKD, and BEAF peaks in differentiated stages of WT and CTCF for Nups. Occupancy heat maps are shown for Nup genes as well as –3 kb and +3 kb around the start and end of Nup genes. Black dashed lines represent the start and end of Nups. The heat maps show the binding of Stwl, BEAF, and CTCF to Nups. The red dashed line delineates the Nups that are downregulated by lfc2. Heat maps show binding of Stwl, BEAF, and CTCF at the TSSs of *nup* genes. (*B*,*B1*) Ovariole of control *nosGAL4* (*B*) and grayscale (*B1*) stained for NPC (red and in grayscale) and DAPI (blue). NPCs form regular ring structures and increase in intensity, leading to the later egg chambers. (*C*,*C1*) Ovariole of *stwl* GKD (*C*) and grayscale (*C1*) stained for NPC (red and in grayscale) and DAPI (blue). NPCs do not increase in intensity, leading to the later egg chambers. (*D*) Arbitrary unit (a.u.) quantification of nucleoporin (Nup) genes in 2 µm × 2 µm egg chambers of *stwl* GKD (red) compared with control ovaries (gray). Statistics were derived from two-tailed *t*-tests. $n = 5$ ovarioles per genotype. (ns) $P > 0.05$, (****) $P < 0.0001$. NPC analysis was done on nurse cells because upon *stwl* depletion, the oocyte was not properly specified, precluding analysis of the oocyte. In addition, nucleoporins synthesized by nurse cells were provided to the oocyte.

lamina, consistent with previous findings (Fig. 7B; Sarkar et al. 2023). However, following *stwl* GKD or in *BEAF* mutants, the *rpS19b* locus was no longer located at the nuclear periphery, indicating its detachment from the lamina (Fig. 7B–G). *BEAF* mutants showed increased fragmentation of the *rps19b* locus, hinting at additional functions. Thus, our results suggest that the NPC, Stwl, and BEAF collectively promote the association of silenced genes with the nuclear lamina, contributing to the maintenance of gene silencing.

Discussion

Germ cell differentiation into an oocyte involves significant changes in gene expression (Flora et al. 2017; DeLuca et al. 2020; Rust et al. 2020; Slaidina et al. 2020; Liang-Yu et al. 2023; Sarkar et al. 2023). Germ cell-specific genes are silenced during this transition, while maternally deposited genes are activated (DeLuca et al. 2020; Sarkar et al. 2023). Active genes tend to be in the nuclear interior, whereas inactive genes are mainly found near the nuclear periphery, close to the lamina (Bank and Gruenbaum 2011; Briand and Collas 2020). The mechanisms that promote such genomic organization during the germ cell-to-maternal transition had not been deciphered.

Here, we found that Stwl accumulates at TAD/LAD boundaries delineating active and repressed genomic compartments during germline differentiation to an oocyte. The presence of Stwl at these boundaries facilitates the establishment of specific chromatin states of these genomic compartments and the maintenance of chromatin marks. Demarcating these compartments is required for both silencing germ cell genes and activating a cohort of maternal genes. In addition, the Stwl-dependent formation of genomic boundaries also promotes the expression of Nups,

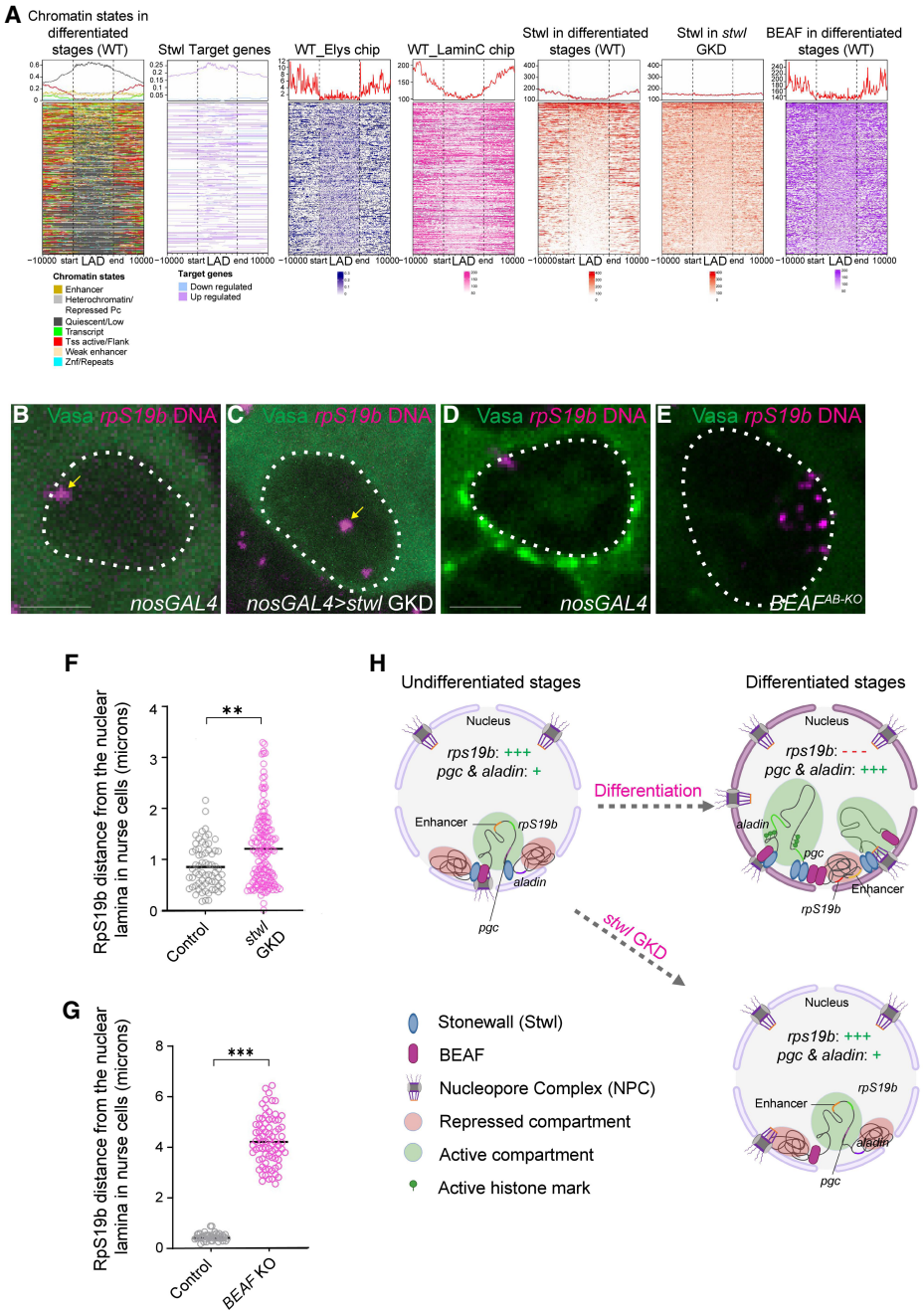

Figure 7. Stwl promotes association of genes to the nuclear periphery. (*A*) CUT&RUN and ChIP occupancy of Stwl, Elys (Nup), Lamin C, and BEAF peaks in differentiated stages of WT ovaries for all LADs. Stwl peaks in differentiated stages are shown in red, Elys from Kc cells is shown in blue, and Lamin C peaks from Lamin C ChIP in S2 cells are shown in pink. Heat maps showing Stwl and Lamin C peak Stwl binding sites as well as −10 kb and +10 kb around the sites. Stwl, Elys, Lamin C, and BEAF all bind on both sides of LADs. (*B*,*C*) Nurse cell nuclei of control (*B*) and *stwl* GKD ovaries (*C*) stained for Vasa (green) and probed for *rpS19b* DNA (magenta). In controls, the *rpS19b* locus is at the nuclear periphery. *stwl* GKD resulted in the migration of the *rpS19b* locus away from the nuclear lamina. (*D*,*E*) Nurse cell nuclei of control (*D*) and *BEAF* KO ovaries (*E*) stained for Vasa (green) and probed for *rpS19b* DNA (magenta). In controls, the *rpS19b* locus is at the nuclear periphery. *BEAF* KO resulted in both fragmentation and the movement of the *rpS19b* locus away from the nuclear lamina. (*F*) *rpS19b* locus distance measured from the nuclear lamina in nurse cells of control WT ovaries and *stwl* GKD ovaries. Distance is measured in micrometers. (Gray) Control ovaries, (pink) *stwl* GKD ovaries. Statistics were derived from unpaired *t*-tests. $n = 4$ ovarioles per control; ovarioles $n = 8$ per *stwl* GKD. (**) $P < 0.01$. (*G*) *rpS19b* locus distance measured from the nuclear lamina in nurse cells of control WT ovaries and *BEAF* KO ovaries. Distance is measured in micrometers. (Gray) Control ovaries, (pink) *BEAF* KO ovaries. The distances of the furthest foci from the periphery were measured. Statistics were derived from unpaired *t*-tests. $n = 4$ ovarioles per control; $n = 8$ ovarioles per *stwl* GKD. (***) $P < 0.001$. (*H*) Model showing that Stwl is required during the transition from undifferentiated stages to differentiated stages of oogenesis to establish boundaries between active and repressed domains by recruiting BEAF to its binding sites and regulating the expression of germ cell differentiation genes and Nups through enhancer dynamics at the nuclear lamina. This model was created with BioRender.com. Scale bars, 15 µm

which aid in the formation of NPCs (Fig. 7H; Hou and Corces 2010). These NPCs in turn tether TADs/LADs to the nuclear lamina, promoting gene regulation (Gonzalez-Sandoval and Gasser 2016). Consistent with Stwl's role in binding NPCs and being present at TAD/LAD boundaries, Stwl is enriched at the nuclear periphery and colocalizes with NPCs (Chavan et al. 2024). Thus, Stwl regulates local and global genome organization to regulate the cell fate transition during oogenesis (Fig. 7H).

Stwl silences early oogenesis genes by demarcating genomic compartments

Stwl is required for GSC maintenance and the proper development of egg chambers (Clark and McKearin 1996). Previously, it had been proposed that Stwl silences differentiation genes potentially via epigenetic control by modulating H3K9me3 and H3K27me3 (Yi et al. 2009; Zinshteyn and Barbash 2022). Indeed, we found that Stwl is critical for silencing early oogenesis genes, some of which promote GSC differentiation into an oocyte (Pritchett et al. 2009). However, we believe that this function of Stwl is not direct. Instead, Stwl plays a crucial role in demarcating silenced and active compartments within the genome in part by recruiting BEAF. By regulating the distribution of these chromatin marks, Stwl indirectly promotes the silencing of early oogenesis genes during oogenesis. This silencing is mediated via modulating the enhancer activity.

The genomic compartments that Stwl demarcates during oogenesis are annotated as TADs or LADs in Kc cells and salivary gland cells (Eagen et al. 2015; Ramírez et al. 2018). The function of TADs has been shown to constrain promoter–enhancer interactions to prevent enhancer capture to regulate proper gene expression (Burgess-Beusse et al. 2002; Cavalheiro et al. 2021; Zuin et al. 2022). It is possible that ectopic expression of repressed genes (such as early oogenesis genes) due to loss of *stwl* could be because of enhancer capture caused by loss of partition between active and repressed chromatin. However, we do not know whether the genomic compartments that we identified during oogenesis are bona fide TADs/LADs during oogenesis. In addition, another caveat is that many of the chromatin changes occurring upon loss of *stwl* could be indirect and simply follow changes in gene transcription rather than being instructive or directly caused by loss of Stwl (Howe et al. 2017).

Stwl not only is required for silencing gene expression but is also critical for activating a cohort of maternally supplied genes such as *pgc* and some *Nup*s (Hanyu-Nakamura et al. 2008; Gozalo and Capelson 2016). We do not think that these maternally provided genes are directly activated by Stwl. Instead, the maternal genes regulated by Stwl are proximal to genomic boundaries that separate active and repressed regions. We think a cohort of maternally supplied genes requires the activity of Stwl to provide a barrier from silenced regions present proximally. While the cohort of maternal genes regulated by Stwl is small compared with the number of genes supplied maternally, it is functionally critical. For example, *pgc* is required to specify a germ cell fate, and Nups are required to complete oogenesis and launch the next generation (Hanyu-Nakamura et al. 2008; Hampoelz et al. 2016; Sarkar et al. 2023). Thus, Stwl coordinates stable silencing of early oogenesis genes to activate maternally provided genes by providing a barrier function between chromatin compartments, preventing the mixing of chromatin states.

Stwl coordinates global genome reorganization by both promoting NPC formation and interacting with NPCs

NPCs are required for global genome organization, but whether global genome organization itself promotes NPC formation was not known (Capelson et al. 2010a; Hou and Corces 2010; Iglesias et al. 2020). Here, we found that by acting as a barrier between active and repressive compartments, Stwl promotes the expression of a cohort of Nups and interacts with them. As all Nups are required for NPC formation, Stwl promotes NPC formation by promoting the transcription of some Nups that comprise the NPC. We previously showed that H3K9me3-mediated chromatin marks are also required for Nup transcription (Sarkar et al. 2023). This suggests that NPC formation is sensitive to both the levels of heterochromatin and how it is demarcated.

NPCs are known to help in a genomic organization by helping both tether silenced genes to the lamina to maintain their silenced state and position active genes under NPCs to allow for RNA export (Capelson et al. 2010b; Ibarra and Hetzer 2015; Gozalo and Capelson 2016; Swati et al. 2023). We show that Stwl colocalizes with NPCs, promoting the anchoring of silenced genes to the nuclear periphery, consistent with the findings of Chavan et al. (2024). We also found that NPC components and Stwl are present at TAD boundaries. Taken together, our data suggest that Stwl, through BEAF recruitment, regulates NPC formation and then, by interaction with NPCs, anchors TADs to the nuclear periphery to maintain their silencing. Indeed, loss of the NPC components *stwl* and BEAF results in loss of Lamin association of an early oogenesis gene, *rpS19b*. Thus, Stwl modulates global genome organization by regulating the formation of and binding to NPCs.

Taken together, we found that Stwl is a critical regulator of local and global genome architecture during the germ cell-to-maternal transition. By establishing boundaries between silenced and active regions, Stwl ensures the confinement of a particular chromatin state and the proper expression of germ cell differentiation genes and Nups to regulate NPC formation. The NPCs in turn promote the tethering of silenced regions to the lamina. This work provides an essential framework for understanding the interplay between genome organization, NPCs, and cell fate determination.

Materials and methods

Fly lines

The following RNAi and mutant fly stocks were used in this study: *stwl* RNAi (Bloomington *Drosophila* Stock

Center [BDSC] 35415); *stwl* deficiency chromosome [*Df (3L)Exel6122*; BDSC 7601]; *stwl* mutants using CRISPR by precise deletions of the open reading sequence (obtained from the Jagannathan laboratory) (Chavan et al. 2024); *stwl* knockout (KO) alleles generated using CRISPR-mediated homology-directed repair, where 1000 bp from the 3′ UTR and 785 bp from the 5′ UTR of Stwl were cloned into a vector (pBSK-attB-DsRed-attB), flanked by a 3XP3-driven DsRed cassette; *bam* RNAi (BDSC 33631); and $BEAF^{AB\text{-}KO}$ mutant flies (obtained from the Hart laboratory).

The following tagged line was used in this study: *rpS19b-GFP* (Buszczak laboratory) (McCarthy et al. 2022).

The germline-specific drivers and double-balancer lines used in this study were *UAS-Dcr2;nosGAL4* (BDSC 25751), *bamGAL4* (BDSC 80579), *matGAL4* (BDSC 7062 and 7063), *nosGAL4;MKRS*/TM6 (BDSC 4442), *If*/CyO; *nosGAL4* (Lehmann laboratory), and *TjGAL4*/*CyO* (Lehmann laboratory).

Reagents for fly husbandry

Fly crosses were grown at 25°C–29°C and dissected between 0 and 3 days after eclosion. Fly food for stocks and crosses was prepared using the Lehman laboratory protocol (summer/winter mix), and narrow vials (Fisherbrand *Drosophila* vials, Fisher Scientific) were filled to ~10–12 mL.

Dissection and immunostaining

Ovaries were dissected, and the ovarioles were separated using mounting needles in PBS solution and kept on ice. Samples were then fixed for 12 min in 5% methanol-free formaldehyde. Ovaries were washed in 0.5 mL of PBT (1× PBS, 0.5% Triton X-100, 0.3% BSA) four times for 10 min each while incubating on a nutator. Primary antibodies in PBT were added and incubated overnight at 4°C while nutating. Samples were next washed three times for 5–8 min each in 1 mL of PBT. Secondary antibodies were added in PBT with 4% donkey serum and incubated for 3–4 h at room temperature. Samples were washed three times for 10 min each in 1 mL of 1× PBST (0.2% Tween 20 in 1× PBS) and incubated in VectaShield with DAPI (Vector Laboratories) for at least 1 h before mounting.

The primary antibodies used were rabbit anti-Stwl 1 (1:2000; obtained from the Jagannathan laboratory), mouse anti-1B1 (1:20; Developmental Studies Hybridoma Bank [DSHB]), rabbit anti-Vasa (1:1000; the Rangan laboratory), chicken anti-Vasa (1:1000; the Rangan laboratory), rabbit anti-GFP (1:2000; Abcam ab6556), rabbit anti-H3K9me3 (1:500; Active Motif AB_2532132), mouse anti-H3K27me3 (1:500; Abcam ab6002), rabbit anti-Egl (1:1000; the Lehmann laboratory), and mouse anti-NPC (1:2000; BioLegend AB_2565026). The following secondary antibodies were used: Alexa 488 (1:500; Molecular Probes), Cy3 (1:500; Jackson Laboratories), and Cy5 (1:500; Jackson Laboratories).

Fluorescence imaging

Ovaries were mounted on slides and imaged using Zeiss LSM-710 and LSM-880 confocal microscopes under 20×, 40×, and 63× oil objectives with pinhole set to one airy unit. Image processing was done using Fiji, and gain adjustment and cropping were performed in Photoshop.

RNA isolation and TURBO

Ovaries were dissected into PBS and transferred to RNase-free microcentrifuge tubes. PBS was removed, 100 µL of Trizol was added, and ovaries were flash-frozen and stored at −80°C. Ovaries were then lysed in the microcentrifuge tubes using a plastic disposable pestle. Trizol was added to 1 mL total volume while vigorously shaking the tubes, and the samples were incubated for 5 min at room temperature. The samples were centrifuged at >13,000*g* for 20 min at 4°C, and the supernatant was transferred to a fresh microcentrifuge tube. Five-hundred microliters of chloroform was added, and the samples were vigorously shaken and incubated for 5 min at room temperature. The samples were spun at maximum speed for 10 min at 4°C. The supernatant was transferred to a fresh microcentrifuge tube and ethanol-precipitated. Sodium acetate was added, equaling 10% of the volume transferred, and 2–2.5 vol of 100% ethanol was added. The samples were shaken thoroughly and left to precipitate overnight at −20°C. The samples were centrifuged at maximum speed for 15 min at 4°C to pellet the RNA. The supernatant was discarded, and 500 µL of 75% ethanol was added to wash the pellet. The samples were vortexed to dislodge the pellet to ensure thorough washing. The samples were spun for 5 min at 4°C, and the supernatant was discarded. The pellets were dried for 10–20 min and then resuspended in 20–50 µL of RNase-free water, and the absorbance at 260 nm was measured on a nanodrop to measure the concentration of each sample.

CUT&RUN assay

Before starting the experiment, stock solutions were prepared and stored: wash buffer (47.5 mL of H_2O, 1 mL of 1 M HEPES at pH 7.5 [final concentration 20 mM], 1.5 mL of 5 M NaCl [final concentration 150 mM], 50 mg of BSA [final concentration 0.1%]), 1× BBT (0.5 g of BSA [final concentration 0.5%], 50 mL of PBST), 2× STOP buffer (46 mL of H_2O, 2 mL of 5 M NaCl [final concentration 200 mM], 2 mL of 0.5 M EDTA [final concentration 20 mM]), 100 mM $CaCl_2$ solution, MXP buffer (10 g of PEG8000 [final concentration 20%], 25 mL of 5 M NaCl [final concentration 2.5 M], 0.5 mL of 1 M $MgCl_2$ [final concentration 10 mM], fill up to 50 mL with H_2O), and permeabilization buffer (50 mL of PBST, 500 µL of Triton-X). On the first experimental day, the wash buffer$^+$ and the BBT$^+$ were freshly prepared and lasted up to 3 days. The wash buffer$^+$ consisted of adding one large Roche complete EDTA-free tablet and 5 µL of 5.55 M spermidine to achieve a final concentration of 0.5 mM, and the BBT$^+$ consisted of adding a large Roche complete EDTA-

free tablet along with 5 µL of 5.55 M spermidine to attain a final concentration of 0.5 mM and 200 µL of 0.5 M EDTA for a final concentration of 2 mM. Following the preparation, 20 pairs of fattened fly ovaries were dissected per replicate and placed on ice in 1× PBS. The sample was then treated with the permeabilization buffer for 1 h at room temperature while nutating, followed by washing with 1 mL of BBT^+ buffer and subsequent removal of the supernatant. Antibody dilutions were then prepared in 500 µL of BBT^+ buffer, and the sample was incubated overnight at 4°C. The next day, the sample was washed with BBT^+ buffer and then incubated with a pAG-MNase 1:100 dilution in 500 µL of BBT^+ for 4 h at room temperature. For DNA cleavage, a $wash^+$ C buffer was prepared by combining 1.5 mL of $wash^+$ buffer with 30 µL of 100 mM $CaCl_2$, followed by resuspending the sample in 150 µL of $wash^+$ C buffer and incubating it for 45 min at 4°C. Next, a 2X STOPyR $buffer^+$ was freshly prepared by adding 1600 µL of 2× STOP buffer and 10 µL of RNase A. At the end of the 45 min incubation, 150 µL of 2× STOPyR buffer was added to the sample and incubated for 30 min at 37°C. The sample was centrifuged at 16,000*g* for 5 min, and the supernatant was carefully extracted and transferred to a fresh Eppendorf tube. To this supernatant, 2 µL of 10% SDS and 2.5 µL of 20 mg/mL Proteinase K were added, and the mixture was thoroughly mixed using a brief vortexing procedure. Subsequently, the sample was incubated in a water bath for a period of 2 h at 50°C. It is important to note that this can be stopped at this step, and the samples can be stored at –20°C. The magnetic beads and MXP were brought to room temperature before proceeding. One-hundred-fifty microliters of the supernatant was extracted for subsequent bead cleanup, while the remainder was kept as a backup. Twenty microliters of AmpureXP bead slurry and 280 µL of MXP buffer were added to the sample and incubated for 15 min at room temperature. Using a magnetic rack, the beads were collected and incubated for 5 min. The supernatant was then discarded. The tubes were kept on the magnet, and 1 mL of 80% ethanol was added to each tube without disturbing the beads. Using a magnetic rack, the beads were collected and incubated for 5 min. The supernatant was then discarded. The tubes were kept on the magnet, and 1 mL of 80% ethanol was added to each tube without disturbing the beads. The sample was then incubated for a minimum of 30 sec, and the ethanol was gently aspirated to remove all traces of ethanol. While the tube remained on the magnet, the beads were air-dried for 2 min and resuspended in 10 µL of RNase-free and DNase-free water. The samples were then incubated for 2 min at room temperature. Following this, the samples were kept on the magnet, and the clear solution was transferred to a new Eppendorf tube. The DNA concentration was determined using a highly sensitive dsDNA Qubit assay, and DNA size distribution in samples was analyzed using a fragment analyzer.

Competing interest statement

The authors declare no competing interests.

Acknowledgments

We thank members of the Rangan laboratory and Dr. Miler T. Lee for their comments on the manuscript. We thank Julia Tang, Shruti Venkat, and Paloma Bravo for help with the HCR protocol. We thank Dr. Kahini Sarkar for help with the cartoon. We thank the Bloomington *Drosophila* Stock Center, Vienna *Drosophila* Resource Center, Berkeley *Drosophila* Genome Project Gene Disruption Project, and FlyBase for reagents and resources. P.R. is funded by the NIH/NIGMS (R01GM111779, RO1GM135628, and R56AG082906). This work was supported in part by the Bioinformatics for Next-Generation Sequencing (BiNGS) shared resource facility within the Tisch Cancer Institute at the Icahn School of Medicine at Mount Sinai, which National Institutes of Health grant P30CA196521 partially supports; the Black Family Stem Cell Institute; and the Department of Cell, Developmental, and Regenerative Biology at the Icahn School of Medicine at Mount Sinai. This work was also supported in part through the computational resources and staff expertise provided by Scientific Computing and Data at the Icahn School of Medicine at Mount Sinai and supported by the Clinical and Translational Science Awards (CTSA) grant UL1TR004419 from the National Center for Advancing Translational Sciences. The research reported here was supported by the Office of Research Infrastructure of the National Institutes of Health under award number S10OD026880.

Author contributions: P.R. and N.M.K. conceived the study. P.R. and N.M.K. performed the methodology. D.H. and G.U. were responsible for the software and performed the formal analysis. D.H., G.U., and N.M.K performed the investigations. P.R. acquired the resources. N.M.K. and G.U. curated the data. P.R. and N.M.K. wrote the original draft of the manuscript. P.R., N.M.K., D.H., G.U., and M.J. reviewed and edited the manuscript. N.M.K. visualized the study. P.R. supervised the study, was the project administrator, and acquired the funding.

References

Ahmad K, Spens AE. 2019. Separate Polycomb response elements control chromatin state and activation of the vestigial gene. *PLoS Genet* **15:** e1007877. doi:10.1371/journal.pgen.1007877

Arzate-Mejía RG, Josué Cerecedo-Castillo A, Guerrero G, Furlan-Magaril M, Recillas-Targa F. 2020. In situ dissection of domain boundaries affect genome topology and gene transcription in *Drosophila*. *Nat Commun* **11:** 894. doi:10.1038/s41467-020-14651-z

Avva SVSP, Hart CM. 2016. Characterization of the *Drosophila* BEAF-32A and BEAF-32B insulator proteins. *PLoS One* **11:** e0162906. doi:10.1371/journal.pone.0162906

Bank EM, Gruenbaum Y. 2011. The nuclear lamina and heterochromatin: a complex relationship. *Biochem Soc Trans* **39:** 1705–1709. doi:10.1042/BST20110603

Bannister AJ, Kouzarides T. 2011. Regulation of chromatin by histone modifications. *Cell Res* **21:** 381–395. doi:10.1038/cr.2011.22

Blatt P, Martin ET, Breznak SM, Rangan P. 2020. Post-transcriptional gene regulation regulates germline stem cell to oocyte

transition during *Drosophila* oogenesis. *Curr Top Dev Biol* **140:** 3–34. doi:10.1016/bs.ctdb.2019.10.003

Blatt P, Wong-Deyrup SW, McCarthy A, Breznak S, Hurton MD, Upadhyay M, Bennink B, Camacho J, Lee MT, Rangan P. 2021. RNA degradation is required for the germ-cell to maternal transition in *Drosophila*. *Curr Biol* **31:** 2984–2994.e7. doi:10.1016/j.cub.2021.04.052

Briand N, Collas P. 2020. Lamina-associated domains: peripheral matters and internal affairs. *Genome Biol* **21:** 85. doi:10.1186/s13059-020-02003-5

Brun S, Rincheval-Arnold A, Colin J, Risler Y, Mignotte B, Guénal I. 2006. The myb-related gene stonewall induces both hyperplasia and cell death in *Drosophila*: rescue of fly lethality by coexpression of apoptosis inducers. *Cell Death Differ* **13:** 1752–1762. doi:10.1038/sj.cdd.4401861

Burgess-Beusse B, Farrell C, Gaszner M, Litt M, Mutskov V, Recillas-Targa F, Simpson M, West A, Felsenfeld G. 2002. The insulation of genes from external enhancers and silencing chromatin. *Proc Natl Acad Sci* **99:** 16433–16437. doi:10.1073/pnas.162342499

Capelson M, Liang Y, Schulte R, Mair W, Wagner U, Hetzer MW. 2010a. Chromatin-bound nuclear pore components regulate gene expression in higher eukaryotes. *Cell* **140:** 372–383. doi:10.1016/j.cell.2009.12.054

Capelson M, Doucet C, Hetzer MW. 2010b. Nuclear pore complexes: guardians of the nuclear genome. *Cold Spring Harb Symp Quant Biol* **75:** 585–597. doi:10.1101/sqb.2010.75.059

Cavalheiro GR, Pollex T, Furlong EE. 2021. To loop or not to loop: what is the role of TADs in enhancer function and gene regulation? *Curr Opin Genet Dev* **67:** 119–129. doi:10.1016/j.gde.2020.12.015

Cavalheiro GR, Girardot C, Viales RR, Pollex T, Cao TBN, Lacour P, Feng S, Rabinowitz A, Furlong EEM. 2023. CTCF, BEAF-32, and CP190 are not required for the establishment of TADs in early *Drosophila* embryos but have locus-specific roles. *Sci Adv* **9:** eade1085. doi:10.1126/sciadv.ade1085

Chavan A, Isenhart R, Nguyen SC, Kotb NM, Harke J, Sintsova A, Ulukaya G, Uliana F, Ashiono C, Kutay U, et al. 2024. A nuclear architecture screen in *Drosophila* identifies Stonewall as a link between chromatin position at the nuclear periphery and germline stem cell fate. *Genes Dev* (this issue) doi:10.1101/gad.351424.123

Chen D, McKearin D. 2003a. Dpp signaling silences bam transcription directly to establish asymmetric divisions of germline stem cells. *Curr Biol* **13:** 1786–1791. doi:10.1016/j.cub.2003.09.033

Chen D, McKearin DM. 2003b. A discrete transcriptional silencer in the bam gene determines asymmetric division of the *Drosophila* germline stem cell. *Development* **130:** 1159–1170. doi:10.1242/dev.00325

Ciabrelli F, Cavalli G. 2015. Chromatin-driven behavior of topologically associating domains. *J Mol Biol* **427:** 608–625. doi:10.1016/j.jmb.2014.09.013

Clark KA, McKearin DM. 1996. The *Drosophila* stonewall gene encodes a putative transcription factor essential for germ cell development. *Development* **122:** 937–950. doi:10.1242/dev.122.3.937

Clough E, Tedeschi T, Hazelrigg T. 2014. Epigenetic regulation of oogenesis and germ stem cell maintenance by the *Drosophila* histone methyltransferase eggless/dSetDB1. *Dev Biol* **388:** 181–191. doi:10.1016/j.ydbio.2014.01.014

Colozza G, Montembault E, Quénerch'du E, Riparbelli MG, D'Avino PP, Callaini G. 2011. *Drosophila* nucleoporin Nup154 controls cell viability, proliferation and nuclear accumulation of Mad transcription factor. *Tissue and Cell* **43:** 254–261. doi:10.1016/j.tice.2011.05.001

Cui J, Sackton KL, Horner VL, Kumar KE, Wolfner MF. 2008. Wispy, the *Drosophila* homolog of GLD-2, is required during oogenesis and egg activation. *Genetics* **178:** 2017–2029. doi:10.1534/genetics.107.084558

Czapiewski R, Robson MI, Schirmer EC. 2016. Anchoring a leviathan: how the nuclear membrane tethers the genome. *Front Genet* **7:** 82. doi:10.3389/fgene.2016.00082

Davis LI, Blobel G. 1987. Nuclear pore complex contains a family of glycoproteins that includes p62: glycosylation through a previously unidentified cellular pathway. *Proc Natl Acad Sci* **84:** 7552–7556. doi:10.1073/pnas.84.21.7552

Dean A, Larson DR, Sartorelli V. 2021. Enhancers, gene regulation, and genome organization. *Genes Dev* **35:** 427–432. doi:10.1101/gad.348372.121

Dekker J, Rippe K, Dekker M, Kleckner N. 2002. Capturing chromosome conformation. *Science* **295:** 1306–1311. doi:10.1126/science.1067799

DeLuca SZ, Ghildiyal M, Pang L-Y, Spradling AC. 2020. Differentiating *Drosophila* female germ cells initiate Polycomb silencing by regulating PRC2-interacting proteins. *Elife* **9:** e56922. doi:10.7554/eLife.56922

Doren MV, Williamson AL, Lehmann R. 1998. Regulation of zygotic gene expression in *Drosophila* primordial germ cells. *Curr Biol* **8:** 243–246. doi:10.1016/S0960-9822(98)70091-0

Eagen KP, Hartl TA, Kornberg RD. 2015. Stable chromosome condensation revealed by chromosome conformation capture. *Cell* **163:** 934–946. doi:10.1016/j.cell.2015.10.026

Ernst J, Kellis M. 2017. Chromatin-state discovery and genome annotation with ChromHMM. *Nat Protoc* **12:** 2478–2492. doi:10.1038/nprot.2017.124

Flora P, McCarthy A, Upadhyay M, Rangan P. 2017. Role of chromatin modifications in *Drosophila* germline stem cell differentiation. In *Signaling-mediated control of cell division: results and problems of cell division* (ed. Arur S), pp. 1–30. Springer, Cham, Switzerland. doi:10.1007/978-3-319-44820-6_1

Galouzis CC, Furlong EEM. 2022. Regulating specificity in enhancer–promoter communication. *Curr Opin Cell Biol* **75:** 102065. doi:10.1016/j.ceb.2022.01.010

Gates LA, Foulds CE, O'Malley BW. 2017. Histone marks in the "drivers seat": functional roles in steering the transcription cycle. *Trends Biochem Sci* **42:** 977–989. doi:10.1016/j.tibs.2017.10.004

Gerbasi VR, Preall JB, Golden DE, Powell DW, Cummins TD, Sontheimer EJ. 2011. Blanks, a nuclear siRNA/dsRNA-binding complex component, is required for *Drosophila* spermiogenesis. *Proc Natl Acad Sci* **108:** 3204–3209. doi:10.1073/pnas.1009781108

Gonzalez-Sandoval A, Gasser SM. 2016. On TADs and LADs: spatial control over gene expression. *Trends Genet* **32:** 485–495. doi:10.1016/j.tig.2016.05.004

Gozalo A, Capelson M. 2016. A new path through the nuclear pore. *Cell* **167:** 1159–1160. doi:10.1016/j.cell.2016.11.011

Gozalo A, Duke A, Lan Y, Pascual-Garcia P, Talamas JA, Nguyen SC, Shah PP, Jain R, Joyce EF, Capelson M. 2020. Core components of the nuclear pore bind distinct states of chromatin and contribute to Polycomb repression. *Mol Cell* **77:** 67–81.e7. doi:10.1016/j.molcel.2019.10.017

Hampoelz B, Mackmull M-T, Machado P, Ronchi P, Bui KH, Schieber N, Santarella-Mellwig R, Necakov A, Andrés-Pons A, Philippe JM, et al. 2016. Pre-assembled nuclear pores insert into the nuclear envelope during early development. *Cell* **166:** 664–678. doi:10.1016/j.cell.2016.06.015

Hanyu-Nakamura K, Sonobe-Nojima H, Tanigawa A, Lasko P, Nakamura A. 2008. *Drosophila* Pgc protein inhibits P-TEFb recruitment to chromatin in primordial germ cells. *Nature* **451:** 730–733. doi:10.1038/nature06498

Hart CM, Cuvier O, Laemmli UK. 1999. Evidence for an antagonistic relationship between the boundary element-associated factor BEAF and the transcription factor DREF. *Chromosoma* **108:** 375–383. doi:10.1007/s004120050389

Herman N, Kadener S, Shifman S. 2022. The chromatin factor ROW cooperates with BEAF-32 in regulating long-range inducible genes. *EMBO Rep* **23:** e54720. doi:10.15252/embr.202254720

Hou C, Corces VG. 2010. Nups take leave of the nuclear envelope to regulate transcription. *Cell* **140:** 306–308. doi:10.1016/j.cell.2010.01.036

Howe FS, Fischl H, Murray SC, Mellor J. 2017. Is H3K4me3 instructive for transcription activation? *Bioessays* **39:** 1–12. doi:10.1002/bies.201600095

Huynh J-R, Johnston DS. 2004. The origin of asymmetry: early polarisation of the *Drosophila* germline cyst and oocyte. *Curr Biol* **14:** R438–R449. doi:10.1016/j.cub.2004.05.040

Ibarra A, Hetzer MW. 2015. Nuclear pore proteins and the control of genome functions. *Genes Dev* **29:** 337–349. doi:10.1101/gad.256495.114

Iglesias N, Paulo JA, Tatarakis A, Wang X, Edwards AL, Bhanu NV, Garcia BA, Haas W, Gygi SP, Moazed D. 2020. Native chromatin proteomics reveals a role for specific nucleoporins in heterochromatin organization and maintenance. *Mol Cell* **77:** 51–66.e8. doi:10.1016/j.molcel.2019.10.018

Januschke J, Gervais L, Dass S, Kaltschmidt JA, Lopez-Schier H, Johnston DS, Brand AH, Roth S, Guichet A. 2002. Polar transport in the *Drosophila* oocyte requires dynein and kinesin I cooperation. *Curr Biol* **12:** 1971–1981. doi:10.1016/S0960-9822(02)01302-7

Kaushal A, Mohana G, Dorier J, Özdemir I, Omer A, Cousin P, Semenova A, Taschner M, Dergai O, Marzetta F, et al. 2021. CTCF loss has limited effects on global genome architecture in *Drosophila* despite critical regulatory functions. *Nat Commun* **12:** 1011. doi:10.1038/s41467-021-21366-2

Kugler J-M, Lasko P. 2009. Localization, anchoring and translational control of oskar, gurken, bicoid and nanos mRNA during *Drosophila* oogenesis. *Fly* **3:** 15–28. doi:10.4161/fly.3.1.7751

Lasko PF, Ashburner M. 1988. The product of the *Drosophila* gene vasa is very similar to eukaryotic initiation factor-4A. *Nature* **335:** 611–617. doi:10.1038/335611a0

Lawrence M, Daujat S, Schneider R. 2016. Lateral thinking: how histone modifications regulate gene expression. *Trends Genet* **32:** 42–56. doi:10.1016/j.tig.2015.10.007

Lehmann R. 2012. Germline stem cells: origin and destiny. *Cell Stem Cell* **10:** 729–739. doi:10.1016/j.stem.2012.05.016

Lesch BJ, Page DC. 2012. Genetics of germ cell development. *Nat Rev Genet* **13:** 781. doi:10.1038/nrg3294

Li MA, Alls JD, Avancini RM, Koo K, Godt D. 2003. The large Maf factor Traffic Jam controls gonad morphogenesis in *Drosophila*. *Nat Cell Biol* **5:** 994–1000. doi:10.1038/ncb1058

Liao Y, Zhang X, Chakraborty M, Emerson JJ. 2021. Topologically associating domains and their role in the evolution of genome structure and function in *Drosophila*. *Genome Res* **31:** 397–410. doi:10.1101/gr.266130.120

Maines JZ, Park JK, Williams M, McKearin DM. 2007. Stonewalling *Drosophila* stem cell differentiation by epigenetic controls. *Development* **134:** 1471–1479. doi:10.1242/dev.02810

McCarthy A, Sarkar K, Martin ET, Upadhyay M, Jang S, Williams ND, Forni PE, Buszczak M, Rangan P. 2022. Msl3 promotes germline stem cell differentiation in female *Drosophila*. *Development* **149:** dev199625. doi:10.1242/dev.199625

McKearin DM, Spradling AC. 1990. bag-of-marbles: a *Drosophila* gene required to initiate both male and female gametogenesis. *Genes Dev* **4:** 2242–2251. doi:10.1101/gad.4.12b.2242

Misteli T. 2020. The self-organizing genome: principles of genome architecture and function. *Cell* **183:** 28–45. doi:10.1016/j.cell.2020.09.014

Mohana G, Dorier J, Li X, Mouginot M, Smith RC, Malek H, Leleu M, Rodriguez D, Khadka J, Rosa P, et al. 2023. Chromosome-level organization of the regulatory genome in the *Drosophila* nervous system. *Cell* **186:** 3826–3844.e26. doi:10.1016/j.cell.2023.07.008

Nakamura A, Amikura R, Mukai M, Kobayashi S, Lasko PF. 1996. Requirement for a noncoding RNA in *Drosophila* polar granules for germ cell establishment. *Science* **274:** 2075–2079. doi:10.1126/science.274.5295.2075

Nallasivan MP, Haussmann IU, Civetta A, Soller M. 2021. Channel nuclear pore protein 54 directs sexual differentiation and neuronal wiring of female reproductive behaviors in *Drosophila*. *BMC Biol* **19:** 226. doi:10.1186/s12915-021-01154-6

Nanni L, Ceri S, Logie C. 2020. Spatial patterns of CTCF sites define the anatomy of TADs and their boundaries. *Genome Biol* **21:** 197. doi:10.1186/s13059-020-02108-x

Navarro C, Puthalakath H, Adams JM, Strasser A, Lehmann R. 2004. Egalitarian binds dynein light chain to establish oocyte polarity and maintain oocyte fate. *Nat Cell Biol* **6:** 427–435. doi:10.1038/ncb1122

Nazer E. 2022. To be or not be (in the LAD): emerging roles of lamin proteins in transcriptional regulation. *Biochem Soc Trans* **50:** 1035–1044. doi:10.1042/BST20210858

Pang L-Y, DeLuca S, Zhu H, Urban JM, Spradling AC. 2023. Chromatin and gene expression changes during female *Drosophila* germline stem cell development illuminate the biology of highly potent stem cells. *Elife* **12:** RP90509. doi:10.7554/eLife.90509

Pathak RU, Sureka R, Bihani A, Varma P, Mishra RK. 2021. In situ nuclear matrix preparation in *Drosophila melanogaster* and its use in studying the components of nuclear architecture. bioRxiv doi:10.1101/2021.09.30.462611

Pritchett TL, Tanner EA, McCall K. 2009. Cracking open cell death in the *Drosophila* ovary. *Apoptosis* **14:** 969–979. doi:10.1007/s10495-009-0369-z

Ramírez F, Bhardwaj V, Arrigoni L, Lam KC, Grüning BA, Villaveces J, Habermann B, Akhtar A, Manke T. 2018. High-resolution TADs reveal DNA sequences underlying genome organization in flies. *Nat Commun* **9:** 189. doi:10.1038/s41467-017-02525-w

Rangan P, DeGennaro M, Jaime-Bustamante K, Coux R-X, Martinho R, Lehmann R. 2009. Temporal and spatial control of germ-plasm RNAs. *Curr Biol* **19:** 72–77. doi:10.1016/j.cub.2008.11.066

Rangan P, Malone CD, Navarro C, Newbold SP, Hayes PS, Sachidanandam R, Hannon GJ, Lehmann R. 2011. piRNA production requires heterochromatin formation in *Drosophila*. *Curr Biol* **21:** 1373–1379. doi:10.1016/j.cub.2011.06.057

Rao SSP, Huntley MH, Durand NC, Stamenova EK, Bochkov ID, Robinson JT, Sanborn AL, Machol I, Omer AD, Lander ES, et al. 2014. A 3D map of the human genome at kilobase resolution reveals principles of chromatin looping. *Cell* **159:** 1665–1680. doi:10.1016/j.cell.2014.11.021

Rowley MJ, Nichols MH, Lyu X, Ando-Kuri M, Rivera ISM, Hermetz K, Wang P, Ruan Y, Corces VG. 2017. Evolutionarily conserved principles predict 3D chromatin organization. *Mol Cell* **67:** 837–852.e7. doi:10.1016/j.molcel.2017.07.022

Roy S, Gilbert MK, Hart CM. 2007. Characterization of BEAF mutations isolated by homologous recombination in *Drosophila*. *Genetics* **176:** 801–813. doi:10.1534/genetics.106.068056

Rust K, Byrnes LE, Yu KS, Park JS, Sneddon JB, Tward AD, Nystul TG. 2020. A single-cell atlas and lineage analysis of the adult *Drosophila* ovary. *Nat Commun* **11:** 5628. doi:10.1038/s41467-020-19361-0

Sarkar K, Kotb NM, Lemus A, Martin ET, McCarthy A, Camacho J, Iqbal A, Valm AM, Sammons MA, Rangan P. 2023. A feedback loop between heterochromatin and the nucleopore complex controls germ-cell-to-oocyte transition during *Drosophila* oogenesis. *Dev Cell* **58:** 2580–2596.e6. doi:10.1016/j.devcel.2023.08.014

Sati S, Cavalli G. 2017. Chromosome conformation capture technologies and their impact in understanding genome function. *Chromosoma* **126:** 33–44. doi:10.1007/s00412-016-0593-6

Seydoux G, Braun RE. 2006. Pathway to totipotency: lessons from germ cells. *Cell* **127:** 891–904. doi:10.1016/j.cell.2006.11.016

Skene PJ, Henikoff S. 2017. An efficient targeted nuclease strategy for high-resolution mapping of DNA binding sites. *Elife* **6:** e21856. doi:10.7554/eLife.21856

Slaidina M, Banisch TU, Gupta S, Lehmann R. 2020. A single-cell atlas of the developing *Drosophila* ovary identifies follicle stem cell progenitors. *Genes Dev* **34:** 239–249. doi:10.1101/gad.330464.119

Spitz F, Furlong EEM. 2012. Transcription factors: from enhancer binding to developmental control. *Nature Reviews Genetics* **13:** 613–626. doi:10.1038/nrg3207

Spradling A. 1993. Germline cysts: communes that work. *Cell* **72:** 649–651. doi:10.1016/0092-8674(93)90393-5

Spradling A, Fuller MT, Braun RE, Yoshida S. 2011. Germline stem cells. *Cold Spring Harb Perspect Biol* **3:** a002642. doi:10.1101/cshperspect.a002642

Stadler MR, Haines JE, Eisen MB. 2017. Convergence of topological domain boundaries, insulators, and polytene interbands revealed by high-resolution mapping of chromatin contacts in the early *Drosophila* melanogaster embryo. *Elife* **6:** e29550. doi:10.7554/eLife.29550

Strambio-De-Castillia C, Niepel M, Rout MP. 2010. The nuclear pore complex: bridging nuclear transport and gene regulation. *Nat Rev Mol Cell Biol* **11:** 490–501. doi:10.1038/nrm2928

Szabo Q, Jost D, Chang J-M, Cattoni DI, Papadopoulos GL, Bonev B, Sexton T, Gurgo J, Jacquier C, Nollmann M, et al. 2018. TADs are 3D structural units of higher-order chromosome organization in *Drosophila*. *Sci Adv* **4:** eaar8082. doi:10.1126/sciadv.aar8082

Talbert PB, Henikoff S. 2021. The yin and yang of histone marks in transcription. *Annu Rev Genomics Hum Genet* **22:** 147–170. doi:10.1146/annurev-genom-120220-085159

Tautz D, Nigro L. 1998. Microevolutionary divergence pattern of the segmentation gene hunchback in *Drosophila*. *Mol Biol Evol* **15:** 1403–1411. doi:10.1093/oxfordjournals.molbev.a025868

Tyagi S, Capitanio JS, Xu J, Chen F, Sharma R, Huang J, Hetzer MW. 2023. High-precision mapping of nuclear pore-chromatin interactions reveals new principles of genome organization at the nuclear envelope. *Elife* **12**. doi:10.7554/eLife.87462

Ulianov SV, Khrameeva EE, Gavrilov AA, Flyamer IM, Kos P, Mikhaleva EA, Penin AA, Logacheva MD, Imakaev MV, Chertovich A, et al. 2016. Active chromatin and transcription play a key role in chromosome partitioning into topologically associating domains. *Genome Res* **26:** 70–84. doi:10.1101/gr.196006.115

Ulianov SV, Doronin SA, Khrameeva EE, Kos PI, Luzhin AV, Starikov SS, Galitsyna AA, Nenasheva VV, Ilyin AA, Flyamer IM, et al. 2019. Nuclear lamina integrity is required for proper spatial organization of chromatin in *Drosophila*. *Nat Commun* **10:** 1176. doi:10.1038/s41467-019-09185-y

van Bemmel JG, Pagie L, Braunschweig U, Brugman W, Meuleman W, Kerkhoven RM, van Steensel B. 2010. The insulator protein SU(HW) fine-tunes nuclear lamina interactions of the *Drosophila* genome. *PLoS One* **5:** e15013. doi:10.1371/journal.pone.0015013

Van Bortle K, Nichols MH, Li L, Ong C-T, Takenaka N, Qin ZS, Corces VG. 2014. Insulator function and topological domain border strength scale with architectural protein occupancy. *Genome Biol* **15:** R82. doi:10.1186/gb-2014-15-5-r82

van Mierlo G, Pushkarev O, Kribelbauer JF, Deplancke B. 2023. Chromatin modules and their implication in genomic organization and gene regulation. *Trends Genet* **39:** 140–153. doi:10.1016/j.tig.2022.11.003

van Steensel B, Belmont AS. 2017. Lamina-associated domains: links with chromosome architecture, heterochromatin and gene repression. *Cell* **169:** 780–791. doi:10.1016/j.cell.2017.04.022

Wharton RP, Struhl G. 1991. RNA regulatory elements mediate control of *Drosophila* body pattern by the posterior morphogen nanos. *Cell* **67:** 955–967. doi:10.1016/0092-8674(91)90368-9

Yang J, Corces VG. 2011. Chromatin insulators: a role in nuclear organization and gene expression. *Adv Cancer Res* **110:** 43–76. doi:10.1016/B978-0-12-386469-7.00003-7

Yang J, Ramos E, Corces VG. 2012. The BEAF-32 insulator coordinates genome organization and function during the evolution of *Drosophila* species. *Genome Res* **22:** 2199–2207. doi:10.1101/gr.142125.112

Yi X, de Vries HI, Siudeja K, Rana A, Lemstra W, Brunsting JF, Kok RM, Smulders YM, Schaefer M, Dijk F, et al. 2009. Stwl modifies chromatin compaction and is required to maintain DNA integrity in the presence of perturbed DNA replication. *Mol Biol Cell* **20:** 983–994. doi:10.1091/mbc.E08-06-0639

Zaccai M, Lipshitz HD. 1996. Differential distributions of two adducin-like protein isoforms in the *Drosophila* ovary and early embryo. *Zygote* **4:** 159–166. doi:10.1017/s096719940000304x

Zinshteyn D, Barbash DA. 2022. Stonewall prevents expression of ectopic genes in the ovary and accumulates at insulator elements in D. melanogaster. *PLoS Genet* **18:** e1010110. doi:10.1371/journal.pgen.1010110

Zuin J, Roth G, Zhan Y, Cramard J, Redolfi J, Piskadlo E, Mach P, Kryzhanovska M, Tihanyi G, Kohler H, et al. 2022. Nonlinear control of transcription through enhancer–promoter interactions. *Nature* **604:** 571–577. doi:10.1038/s41586-022-04570-y

Zullo JM, Demarco IA, Piqué-Regi R, Gaffney DJ, Epstein CB, Spooner CJ, Luperchio TR, Bernstein BE, Pritchard JK, Reddy KL, et al. 2012. DNA sequence-dependent compartmentalization and silencing of chromatin at the nuclear lamina. *Cell* **149:** 1474–1487. doi:10.1016/j.cell.2012.04.035